





Spatiotemporal Evolution and Driving Mechanism of Fractional Vegetation Coverage in the Yangtze River Delta

Xueru Tian , Zui Tao , Yong Xie , Senior Member, IEEE, Wen Shao , and Shiyu Zhang

Abstract—An in-depth exploration of fractional vegetation coverage (FVC) changes and driving mechanisms in the Yangtze River Delta (YRD) is crucial for maintaining regional ecological health and achieving sustainable development. We therefore calculate FVC in the YRD from 2012 to 2021 based on MODIS NDVI data, and analyze its spatiotemporal evolution. Multiple regression residual analysis and geographic detector model were used along with various auxiliary data to further explore its driving mechanisms in a hierarchical manner. Finally, the Hurst index was used to forecast future trends in FVC. The results show that: 1) Significant changes in FVC occurred around 2016, rapidly declining at a rate of $8.9 \times 10^{-3} \text{a}^{-1}$ from 2012 to 2016, followed by fluctuating growth at a rate of $5.2 \times 10^{-3} \text{a}^{-1}$ thereafter. 2) Although the overall development of FVC in the YRD tends toward stability, the fluctuation was pronounced in the Taihu Lake Basin. Improvement areas were mainly concentrated on both sides of the Yangtze River in the central part of the YRD and in the southern mountainous region. Degraded areas were concentrated in cities north of the Huai River. 3) Dynamic changes in FVC were primarily driven by a combination of climate and human activities, whereas spatial heterogeneity was mainly driven by factors such as elevation, slope, and landform type. The improvement in the explanatory power of anthropogenic factors for spatial heterogeneity when combined with natural factors was significant.

Index Terms—Driving mechanism, fractional vegetation coverage, spatiotemporal evolution, Yangtze River Delta.

I. INTRODUCTION

VEGETATION covers approximately 20% of the Earth's surface and plays a crucial role in responding to climate change, soil and water conservation, and carbon neutrality [1], [2], [3], [4]. Vegetation growth condition is a key indicator for monitoring and evaluating changes in ecology [5]. This growth condition also reflects the positive and negative responses of

Manuscript received 27 February 2024; revised 28 April 2024; accepted 16 May 2024. Date of publication 31 May 2024; date of current version 14 June 2024. This work was supported in part by the National Natural Science Foundation of China under Grant 42176176; in part by the National Key Research and Development Program of China under Grant 2023YFB3905801; and in part by the Land Observation Satellite Supporting Platform of National Civil Space Infrastructure Project. (Corresponding author: Yong Xie.)

Xueru Tian, Yong Xie, Wen Shao, and Shiyu Zhang are with the School of Geographical Sciences, Nanjing University of Information Science and Technology, Nanjing 210044, China (e-mail: 202212100010@nuist.edu.cn; xieyong@nuist.edu.cn; wenshao@nuist.edu.cn; 202212100026@nuist.edu.cn).

Zui Tao is with the Aerospace Information Research Institute Chinese Academy of Sciences, Beijing 100094, China (e-mail: taozui@aircas.ac.cn).

Digital Object Identifier 10.1109/JSTARS.2024.3407727

human beings to their natural environment [6], [7], [8]. Focusing on the changes in vegetation and its connection with the external environment can assist timely realize the survival status and development needs of vegetation in a region, accordingly adjust the relevant policies, and improve the ecological health of the region [9]. Therefore, discussion on the process and driving mechanism of vegetation dynamic change has become a hot topic in academic research.

Fractional vegetation coverage (FVC) refers to the percentage of the vertical projection area of vegetation (including leaves, stems, and branches) to the total area of the study area [10], which is an excellent indicator for describing vegetation growth condition and reflecting the evolution of the ecological environment [11]. It has been widely used in the monitoring of vegetation dynamics with the remote sensing technology [12]. Rouse et al. [13] concluded that the normalized difference vegetation index (NDVI) is sensitive to the vegetation growth condition and spatial heterogeneity, has a strong resistance to the interference of atmospheric and topographic. Therefore, it has an obvious advantage in large-scale monitoring of vegetation dynamics [14], [15], [16]. NDVI and FVC show a significant linear relationship [17]. Yuan et al. [18] estimated the FVC in western China based on NDVI and further analyzed its spatiotemporal variation characteristics. Yang et al. [19] used NDVI to obtain FVC information in the Amur River Basin, and on this basis, combined with climate data, and explored its influencing factors. Currently, NDVI has become the most widely used vegetation index in FVC research [20], [21], [22]. Therefore, we used the dimidiate pixel model to estimate FVC based on MODIS NDVI data, and combined it with the center of gravity transfer model, Theil-Sen median analysis, and coefficient of variation, to investigate the spatiotemporal evolution characteristics of FVC in the YRD from 2012 to 2021.

Climate is one of the dominant factors influencing the growth of surface vegetation, especially where changes in precipitation and temperature directly impact plant photosynthesis, respiration, and the rate of decomposition of organic matter in the soil, which further leads to changes in the dynamics of FVC [14], [23]. Current research on the driving mechanisms of FVC focuses on analyzing the effects of the climate change on FVC dynamics [24]. For example, Liu et al. [17] analyzed the effects of climate factors on FVC in subtropical China from 2001 to 2018. The results showed that the annual average minimum

temperature had the greatest impact on the region. Jia et al. [25] combined climate factors to analyze the dynamic changes in FVC in the Ordos region, Inner Mongolia, from 1982 to 2015, and found a significant difference in the sensitivity of FVC to changes in various climate elements. Although the current study shows that there is a strong correlation between FVC changes and climate factors and there are obvious spatial differences in the response of FVC changes to climate change, vegetation growth is often affected by many aspects from the natural environment and human activities [26]. Sun et al. [27] found that meadow degradation in the Tibetan Plateau region became serious because of overgrazing; Li et al. [28] found that because of the implementation of a series of ecological construction projects such as afforestation and conversion of farmland back to forests and grassland, the FVC in the Loess Plateau and Ordos in the Yellow River Basin showed a gradual increase after 2000. Therefore, the effects of both climatic factors and influence of human activities should be considered on the change of FVC [29]. Compared with studies on the effects of dynamic changes, spatial heterogeneity of FVC has received less attention. However, understanding the driving mechanism behind the spatial variability of FVC can help formulate the relevant vegetation protection policies and further improve the vegetation survival. Some scholars made contributions in this area, however, they lacked comprehensiveness in factor selection. For example, Wu et al. [20] explored the causes of FVC spatial heterogeneity in the three northeastern provinces by combining climatic background data and human activity data, such as population, GDP, and land-use types. However, these data lacked nonclimatic natural factors, such as geomorphic and soil types, in factor selection.

Core developed areas help maintain the health of regional ecological civilization and establishing interregional ecological compensation mechanism. However, so far, studies related to FVC in developed areas in China are significantly less than those in ecologically vulnerable and functional areas [21], [30]. The Yangtze River Delta (YRD) is one of China's economic core areas; therefore, an in-depth investigation of its FVC changes and driving mechanisms is of practical significance for regional ecological protection and integrated green development. However, the current studies on FVC in this region similarly mostly focus on analyzing the response of single types of factors, such as climate, to changes in its dynamics. Cui et al. [31] explored the correlation between the change in vegetation greenness in the YRD and precipitation and temperature from 2001 to 2013; Wang et al. [32] discussed the impact of the climate change on FVC in the YRD based on the Google Earth Engine platform. The research process has not explored the impacts of human activities such as urban expansion and economic development on the rapid changes in the YRD and not analyzed the spatial heterogeneity of FVC. Therefore, it is considered that the mechanism of FVC driving force in this region is not explored in depth. In addition, the future development of FVC in the YRD did not receive attention, which is not conducive to the preventive protection of vegetation in the region.

Considering the current research status of FVC in YRD, this study divided the relevant driving factors into three categories: climatic natural factor, nonclimatic natural factor, and human

activity factor. We defined climatic natural factor and human activity factor as dynamic factor, and nonclimatic natural factor as relatively static factor. We argued that the dynamic changes in FVC were mainly driven by the dynamic factor changes and spatial heterogeneity was driven by the distribution of mean values of the relatively static factor and dynamic factor. It was believed that the dynamic changes of FVC are mainly driven by the changes of dynamic factor, while the spatial heterogeneity was driven by the distribution of mean value of relative static and dynamic factor. A hierarchical exploration of the FVC driving mechanism makes the study more comprehensive and in-depth. Multiple regression residual analysis can effectively separate the effects of climate and human activities [33]. After further processing, such analysis can quantify the single and coupled influences of the two types of factors on the dynamic changes of FVC in the YRD. However, the geographic detector model can effectively detect the spatial heterogeneity of FVC and reveal the driving mechanism behind it [34], [35]. The problem of linear and normal distribution of the data can be ignored [36]. Therefore, based on MODIS NDVI data, we used multiple regression residual analyses and the geographic detector model to discuss the driving force mechanism of FVC in YRD, and coupled the results of the Hurst index and FVC trends test to predict the future development trend of the region to provide a more comprehensive and in-depth analysis of FVC in the YRD region.

The objectives of this study were

- 1) to analyze the spatial and temporal evolution characteristics and future development trends of FVC in the YRD;
- 2) to determine the driving mechanisms of FVC dynamics; and
- 3) to assess the key driving forces of spatial heterogeneity of FVC and the impacts arising from the interactions of the factors, and explore the appropriateness of FVC at various levels or types of the same driving force.

MODIS NDVI data enable us to monitor the dynamics of FVC efficiently over long time series by further combining it with data from multiple correlation factors. The results of this study can provide insight into the evolutionary pattern of FVC in the YRD and comprehensively analyze its driving mechanisms. It is expected to provide effective information for protecting the ecological health of the YRD and promoting the coordinated development of the economy, society, and natural environment.

II. MATERIALS AND METHODS

A. Study Area

The YRD is located in the coastal area of east-central China, in the lower reaches of the Yangtze River, and consists of three provinces, Jiangsu, Zhejiang, Anhui, and Shanghai, with 41 prefectural cities. Its latitude and longitude ranges are 27°–35°N, 114°–123°E, with a total area of approximately 358,000 square kilometers (see Fig. 1). The region features a complex terrain, including plains, hills, plateaus, and mountains, with the terrain gradually decreasing from southwest to northeast. Simultaneously, the ecosystem of the region is diverse, comprising various vegetation types such as coniferous forests, broad-leaved forests,

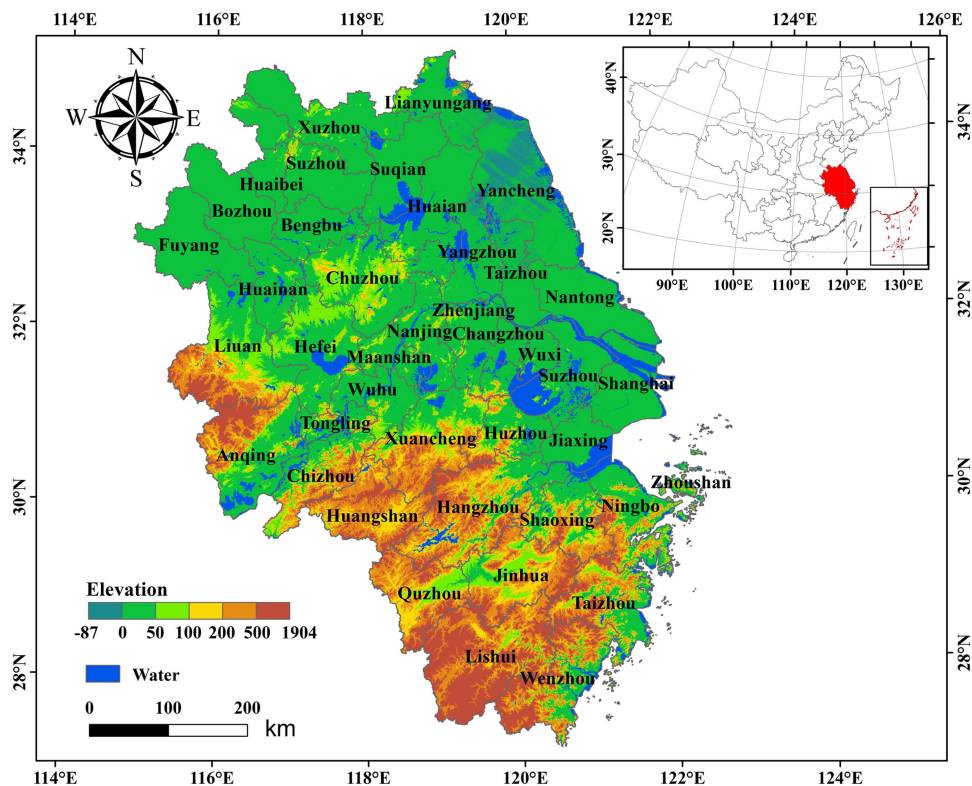


Fig. 1. Location and topography of the Yangtze River Delta (YRD).

shrubs, grasslands, meadows, and cultivated vegetation. Being predominantly situated in the East Asian monsoon region south of the Qinling Mountains–Huai River, the region is dominated by a subtropical monsoon climate [32]. Its characteristics include hot and rainy summers and cold and dry winters, with an average annual temperature of 15–17°C [37]. The annual average precipitation decreases from southeast to northwest, with the plum rain season mainly occurring in June and July, lasting approximately 20–30 days [38]. Heavy rainfall, floods, and debris flows can occur during the summer and autumn seasons [39]. The overall economic development of the YRD shows a distribution trend decreasing in a stepped manner, with Shanghai as the core. This region exhibits evident spatial aggregation characteristics, with uneven development among various cities.

Because of the complex terrain, diverse vegetation, frequent natural disasters, and uneven economic development in this region, significant differences exist in the conditions for vegetation survival, posing challenges for conservation and management. Therefore, a thorough investigation into the dynamic changes and driving mechanisms of FVC in the YRD is crucial. This exploration holds significant importance in enhancing the supply capacity of ecosystem services and promoting the integrated green and coordinated development of the YRD.

B. Basic Data and Preprocessing

The 2012–2021 NDVI data for the growing season (April to October) in the YRD used in this study were obtained from the MOD13Q1 NDVI dataset. These data were provided by LAADS

DAAC with a temporal resolution of 16 days and a spatial resolution of 250 m. The raw NDVI data were preprocessed using the MODIS Reprojection Tool (MRT) for format conversion, reprojection, and stitching. To eliminate disturbances from cloud cover, atmospheric conditions, and solar zenith angles, the maximum value compositing (MVC) method was used to obtain monthly NDVI data [40]. The monthly NDVI data were then averaged to obtain the yearly NDVI dataset (to improve the accuracy of FVC inversion, water was removed using the MOD12Q1 data from 2012).

The night-time light data were provided by National Oceanic and Atmospheric Administration. During the processing of these data, considering the humid and cloudy conditions of the YRD in summer, where cloud cover significantly affects its quality, we selected data from September and October and aligned the information with the vegetation growth period. Following the processing methods proposed by Wu et al. [41], we synthesized a dataset of night-time light data from 2012 to 2021 in the YRD.

The DEM was obtained from the SRTMDEMUTM 90M dataset from the Geospatial Data Cloud. Using ArcGIS 10.2, surface analysis was conducted on the DEM data to extract slope and aspect. The landform, vegetation, and soil type data were sourced from the 1:1,000,000 thematic map classification provided by the Resource and Environment Science and Data Center. The climate data were obtained from the CRU TS v.4.07 dataset provided by the Climate Research Unit gridded Time Series.

The above data were summarized in Table I and projected and sampled for consistency with the NDVI data.

TABLE I
DATA SOURCES

Type	Index	Spatial resolution	Temporal resolution	Source
Vegetation	NDVI	250 m×250 m	16 days	LAADS DAAC
Land use	LUCC	500 m×500 m	Yearly	(https://ladsweb.modaps.eosdis.nasa.gov/)
Human activity factor	Night-time light	1000 m×1000 m	Monthly	National Oceanic and Atmospheric Administration (https://www.noaa.gov/)
Non-climatic natural factors	Elevation	90 m×90 m	-	Geospatial Data Cloud (https://www.gscloud.cn/)
	Slope		-	
	Aspect	1000 m×1000 m	-	Resource and Environment Science and Data Center (https://www.resdc.cn/)
	Landform		-	
Climatic natural factors	Vegetation types	1000 m×1000 m	-	Climatic Research Unit gridded Time Series (https://crudata.uea.ac.uk/cru/data/hrg/)
	Soil types		-	
	Annual average precipitation		Monthly	
	Annual average temperature			

TABLE II
GRADES OF FVC IN THE YRD

Value	Fractional vegetation cover grade
< 10%	Low FVC
10%–30%	Medium low FVC
30%–50%	Medium FVC
50%–70%	Medium high FVC
>70%	High FVC

TABLE III
DETECTING TRENDS IN FVC IN THE YRD

β	Z	Degree of change
>0	≥ 1.96	Significant increase
	<1.96	Slight increase
=0	=0	Insignificant change
	≥ 1.96	Slight decrease
<0	<1.96	Significant decrease

C. Main Methods

1) *FVC Estimation*: In this study, the dimidiate pixel model was used to calculate the FVC in the YRD. The model assumes that each pixel contains only pure vegetation information and pure soil information [17], and the proportion of the pixel area that has vegetation cover is the FVC of the pixel. The formula is as follows:

$$FVC_i = (NDVI_i - NDVI_{soil}) / (NDVI_{veg} - NDVI_{soil}) \quad (1)$$

where i is the pixel, $NDVI_i$ denotes the NDVI value of the i th pixel, $NDVI_{veg}$ denotes the NDVI value of the pure vegetation pixel, $NDVI_{soil}$ denotes the NDVI value of the pure bare soil pixel, and FVC_i is the fractional vegetation cover of the i th pixel.

Theoretically, $NDVI_{veg}$ should be close to 1 and $NDVI_{soil}$ should be close to 0. However, the actual values of $NDVI_{veg}$ and $NDVI_{soil}$ differ because of many factors, such as weather conditions, spatial and temporal variation and vegetation types [42]. In this study, $NDVI_{veg}$ and $NDVI_{soil}$ values were selected using a confidence interval of 1%–99% for the estimation of FVC in the study area. Based on the previous experience [20] and combined with the actual distribution of vegetation in the YRD, FVC was classified into classes (see Table II).

2) *Center of Gravity Transfer Model*: The center of gravity transfer model can be used to analyze the spatial change trajectory of an element [43]. In this study, we used this model to explore the migration characteristics of the FVC. The formula was as follows:

$$X_t = \frac{\sum_{i=1}^n (C_{it} \times X_{it})}{\sum_{i=1}^n C_{it}} \quad (2)$$

$$Y_t = \frac{\sum_{i=1}^n (C_{it} \times Y_{it})}{\sum_{i=1}^n C_{it}} \quad (3)$$

where X_t is the longitudinal coordinates of the center of gravity for various FVC grades and Y_t is the latitudinal coordinates. C_{it} denoted the area of the i th FVC patch in the t -year and X_{it} and Y_{it} represent the longitude and latitude coordinates of the center of gravity of the i th FVC patch in the t th year.

3) *Theil–Sen Median Analysis and Mann–Kendall Test*: Theil–Sen median analysis is computationally efficient and insensitive to outliers, representing a robust nonparametric trend calculation method [44]. This approach was used to analyze the interannual variation trends in FVC. The formula was as follows:

$$\beta = \text{median} \left(\frac{FVC_i - FVC_j}{i - j} \right) \quad (4)$$

where β is the trend of FVC; FVC_i and FVC_j are the FVC values in the i th and j th years, respectively ($1 < i < j < n$). When $\beta > 0$, FVC shows an increasing trend; and when $\beta < 0$, FVC shows a decreasing trend.

The results of the Theil–Sen median analysis were tested for trend significance using the Mann–Kendall test, and the combination of the two methods improved the accuracy of the results to some extent [45].

Theil–Sen median analysis and Mann–Kendall test results were classified into five types (see Table III).

4) *Coefficient of Variation*: The coefficient of variation was used to describe the degree of volatility in the long-time series FVC [21]. The formula was as follows:

$$CV = \frac{1}{FVC} \sqrt{\frac{\sum_{i=1}^n (FVC_i - FVC)^2}{n-1}} \quad (5)$$

TABLE IV
STABILITY OF FVC IN THE YRD

CV	Degree of fluctuation
<0.05	Low fluctuation
0.05–0.10	Relatively low fluctuation
0.10–0.15	Moderate fluctuation
0.15–0.20	Relatively high fluctuation
>0.20	High fluctuation

TABLE V
ORIENTATION OF CLIMATE AND HUMAN ACTIVITY CHANGES TO THE DYNAMIC CHANGES OF FVC

Slope (FVC _{CC/HA})	Type of impact
<-0.02	Degradation
-0.02–0.02	Steadily
>0.02	Improvement

where CV is the coefficient of variation of FVC for a long-time series; n is the length of the time series; FVC_i is the value of FVC at the i th year; and \overline{FVC} is the mean value of FVC during the study period. A higher CV value indicates that the time series is more unstable. In contrast, this value also indicates that the time series is more stable.

The detection results were shown in Table IV.

5) *Multiple Regression Residual Analysis*: Multiple regression residual analyses were used to investigate the effects of the climate change and human activities on FVC changes [33]. The formula was as follows:

$$FVC_{CC} = a \times T + b \times P + c \quad (6)$$

$$FVC_{HA} = FVC_{OBS} - FVC_{CC} \quad (7)$$

where FVC_{CC} , FVC_{OBS} , and FVC_{HA} refer to the predicted value of FVC, the observed value of FVC based on remote sensing images, and the residual value of FVC, respectively; a , b , and c are the model parameters; and T and P refer to the average temperature and precipitation during the vegetation growing season, respectively. FVC_{CC} and FVC_{HA} reflect the impacts of climate and human activity on FVC, respectively.

To further evaluate the influence orientation of climate and human activity on the dynamic changes of FVC in the YRD, the influence of the two factors was further divided according to the trends of FVC_{CC} and FVC_{HA} [29], and the results of the division were shown in Table V.

In addition, the main driver factors of FVC dynamics were distinguished according to Table VI, and the relative contribution of the two factors to FVC dynamics was calculated.

6) *Geographic Detector Model*: The geographic detector is a novel statistical method used in vegetation research to identify spatial heterogeneity and uncover the underlying driving mechanisms [46]. Drawing from previous studies [20], [47], [48], [49], [50], this study selected eight natural factors and

one human activity factor (see Table VII) to investigate their respective influences on FVC within the study area.

The actual situation in the study area and the characteristics of each factor were considered to grade the factor data. The natural breakpoint method was employed to classify the annual average night light value and slope into five classes, whereas the DEM, annual average temperature, and annual precipitation were categorized into nine classes. In addition, the aspect was classified into ten classes, based on the results of aspect direction analysis conducted using ArcGIS 10.2. With reference to the 1:1000,000 thematic map classification provided by the Resource and Environment Science and Data Center, the landform types of the study area were classified into four classes: plain, platform, and others; vegetation types were classified into eight classes: coniferous forest, broadleaved forest, cultivated vegetation and others; and soil types were classified into nine classes: saline-alkali soil, primary soil and others. The data of each factor type and the annual average FVC in the YRD were extracted from the sampling points, and the corresponding data of each sampling point were imported into the geographic detector software for processing.

a) *Factor detector*: The factor detector focuses on exploring the impact of various factors on the spatial heterogeneity of FVC, i.e., the explanatory power of the independent variable X on the dependent variable Y [51]

$$q = 1 - \frac{\sum_{h=1}^L N_h \sigma_h^2}{N \sigma^2} = 1 - \frac{SSW}{SST} \quad (8)$$

$$SSW = \sum_{h=1}^L N_h \sigma_h^2 \quad (9)$$

$$SST = N \sigma^2 \quad (10)$$

where q range is [0, 1], representing the contribution of the examined factor to heterogeneity in FVC. A higher q value signifies a stronger explanatory power of the examined factor for FVC, and the converse is also true. $h = 1, 2, \dots, L$ denotes the stratification of either the dependent variable FVC or the independent variable, detected factor; N_h and N correspond to the unit count in layer h and for the entire region, respectively; σ_h^2 and σ^2 stand for the variance of FVC within layer h and for the entire region, respectively. Finally, SSW and SST represent the total variance within each layer and for the entire region, respectively.

b) *Interaction Detector*: The interaction detector is suitable for detecting the interaction between various factors, i.e., evaluating whether the explanatory power of the spatial heterogeneity of the dependent variable FVC changes under the interaction of two factors [36].

- 1) Nonlinear weakness: $q(X_i \cap X_j) < \min [q(X_i), q(X_j)]$;
- 2) Single-factor nonlinear weakness: $\min [q(X_i), q(X_j)] < q(X_i \cap X_j) < \max [q(X_i), q(X_j)]$;
- 3) Independent: $q(X_i \cap X_j) = q(X_i) + q(X_j)$;
- 4) Two-factor enhancement: $q(X_i \cap X_j) > \max [q(X_i), q(X_j)]$;
- 5) Nonlinear enhancement: $q(X_i \cap X_j) > q(X_i) + q(X_j)$.

TABLE VI
DETERMINATION OF DRIVERS OF DYNAMIC CHANGE AND CALCULATION OF RELATIVE CONTRIBUTIONS

Slope (FVC _{CC/HA})	Type of impact	Identification criterion		Relative contribution rate (%)	
		Slope (FVC _{CC})	Slope (FVC _{HA})	Climate change	Human activity
>0	Jointly promotion	>0	>0	$\frac{Slop(FVC_{CC})}{Slop(FVC_{obs})}$	$\frac{Slop(FVC_{HA})}{Slop(FVC_{obs})}$
	Climate promotion	>0	<0	100	0
	Human promotion	<0	>0	0	100
<0	Jointly inhibition	<0	<0	$\frac{Slop(FVC_{CC})}{Slop(FVC_{obs})}$	$\frac{Slop(FVC_{HA})}{Slop(FVC_{obs})}$
	Climate inhibition	<0	>0	100	0
	Human inhibition	>0	<0	0	100

TABLE VII
SELECTION OF FACTORS INFLUENCING FVC IN THE YRD

Factor	Index	Unit
X1	Night time light	nW/cm ² /sr
X2	Elevation	m
X3	Slope	°
X4	Aspect	°
X5	Landform	-
X6	Vegetation	-
X7	Soil	-
X8	Annual average precipitation	mm
X9	Annual average temperature	°C

TABLE VIII
FORECAST OF FUTURE DEVELOPMENT OF FVC IN THE YRD

H	β	The type of future development trend
0–0.5	>0	From increase to decrease
	<0	From decrease to increase
=0.5	=0	Not significant
0.5–1	>0	Continuous improvement
	<0	Continuous degradation

c) *Risk Detector*: Risk detector is suitable for detecting a suitable type or range of different factors on FVC, which is tested by *t*-statistics [52]

$$t_{\bar{y}_{h=1}-\bar{y}_{h=2}} = \frac{\bar{Y}_{h=1}-\bar{Y}_{h=2}}{\left[\frac{Var(\bar{Y}_{h=1})}{n_{h=1}} + \frac{Var(\bar{Y}_{h=2})}{n_{h=2}}\right]^{\frac{1}{2}}} \quad (11)$$

where n_h represents the number of samples of detected factors in layer h ; \bar{Y}_h represents the mean value of the FVC change trend of the detected factors in layer h and Var represents variance.

7) *Hurst Index*: The Hurst index was used to analyze the future development trend of FVC, wherein the main principle is to construct a time series {FVC(t)}, $t = 1, 2, \dots, n$, for any positive integer, $T = 1, 2, \dots$, define the mean series as

$$\overline{FVC(T)} = \frac{1}{T} \sum_{t=1}^T FVC(t) \quad (12)$$

$$X(t, T) = \sum_{t=1}^T (FVC(t) - \overline{FVC(T)}) \quad (13)$$

$$R(T) = \max X(t, T) - \min X(t, T) \quad (14)$$

$$S(T) = \left[\frac{1}{T} \sum_{t=1}^T (FVC(t) - \overline{FVC(T)})^2 \right]^{\frac{1}{2}} \quad (15)$$

where $X_{(t,T)}$ is the cumulative deviation between the time series and its mean; $R_{(T)}$ is the range of cumulative deviation; and $S_{(T)}$ is the standard deviation of the time series.

Referring to existing results [20], Hurst results were classified into three categories: $0 < H < 0.5$, no sustainability; $H = 0.5$, uncertain sustainability trend; $0.5 < H < 1$, sustainability. To better understand the future development of FVC in the study area, the Hurst index results were coupled with the Theil–Sen median analysis. The results were classified into five classes (see Table VIII).

III. RESULTS

A. Temporal Variation Characteristics of the FVC

Using linear regression analysis on the annual average FVC from 2012 to 2021 in the YRD (see Fig. 2), the results indicate that the annual average FVC of the YRD remained between 0.61 and 0.67 throughout the study period. The highest FVC occurred in 2014 at 0.6612, whereas the lowest is in 2016 at 0.6153. The change in the FVC can be divided into two phases: before 2016, the FVC show a rapid decline at a rate of $8.9 \times 10^{-3} a^{-1}$, whereas after 2016, the FVC exhibit a fluctuating upward trend at a rate of $5.2 \times 10^{-3} a^{-1}$.

From Fig. 3, complex transitions occurred between various FVC grades in various time periods in the YRD (to clearly demonstrate the transition process; only the transitioning parts are represented in the figure). Overall, the most intense transitions occurred in the medium high FVC categories, with this level being the most involved in transitions among the three time periods considered. In contrast, transitions in low FVC

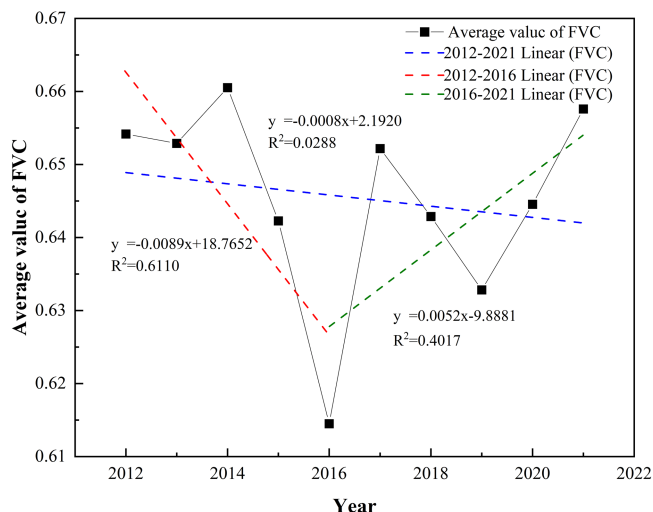


Fig. 2. Average annual FVC change trend in the YRD from 2012 to 2021.

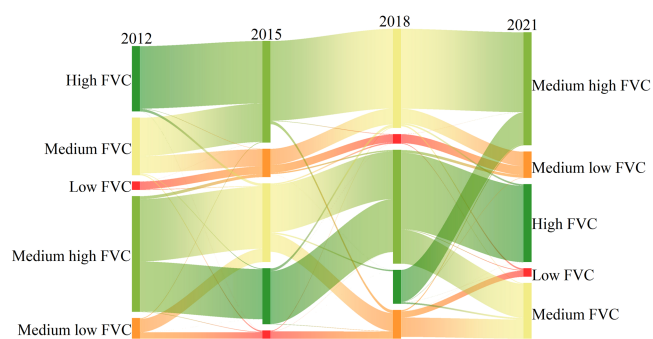


Fig. 3. Sankey of FVC grade transfer in YRD from 2012 to 2021.

are weaker, with slight changes. Combining Figs. 2 and 3, and analyzing various time periods reveals the following: from 2012 to 2015, a relatively pronounced downward trend in FVC is observed, primarily because of a substantial shift from the high and medium high FVC to the next lower level. Although there are significant areas transitioning from medium high to high grades, this is not enough to alter the overall declining trend. From 2015 to 2018, the transition tendency in the high FVC weakened compared with that of the previous phase, with a predominant flow from medium-high to medium FVC. At the same time, medium FVC experience a reverse supplement, resulting in no significant change in the annual average. Finally, from 2018 to 2021, the outflow of high and medium high FVC has been reduced, accompanied by other grades of large-scale transfer in. Although there is a significant increase from transitions in the medium low grade to the lower grade compared with the previous periods, its overall impact remains minimal, leading to a notable increase in the overall coverage.

B. Spatial Distribution Characteristics of the FVC

From 2012 to 2021, the FVC within the YRD exhibited significant spatial heterogeneity, characterized by an overall distribution pattern of high in the west and low in the east, with

high in the north and south, however, low in the central parts (see Fig. 4). Combining Figs. 4 and 5, the area proportion of medium, medium low, and low FVC has fluctuated little between ten years and basically expanded or decreased depending on the original areas. The regions with significant changes of these three grades are mainly distributed along the Yangtze River. The proportion of high and medium high FVC is in a state of inverse correlation, and the change is concentrated in northern Jiangsu, especially in Yancheng, Lianyungang, and Huai'an. From Fig. 6, examining the average spatial distribution of FVC grades reveals that the area with the medium high FVC occupies the largest, accounting for 41.46% of the total, primarily located in the northern and central regions of Anhui Province and the central area of Jiangsu Province. The next important area is characterized by the high FVC, representing 39.40% of the total area and mainly situated in the central and southern parts of Zhejiang Province, northern Jiangsu Province, and the southern parts of Anhui Province. Medium, medium low, and low FVC areas constitute smaller proportions of the study area, accounting for 12.01%, 5.35%, and 1.78%, respectively. They are mainly distributed in Shanghai, southern Jiangsu, and northern Zhejiang.

This study employs the center of gravity transfer model to quantitatively express the migration characteristics of FVCs based on the classification of FVC grades in Table II. The results (see Fig. 7) indicate that during the study period, the gravity center of low FVC was situated in the area between Changzhou and Wuxi. The migration direction is first to the southwest and then to the northeast, initially moving from the southern part of Wuxi to the southern part of Changzhou and then experiencing a return migration. The gravity center of medium low FVC was in the area adjacent to Nanjing and Changzhou. The migration direction was first to the west and then to the southeast. The gravity center of medium FVC was also in the Nanjing area, with the migration direction was first to the northwest and then to the southeast, gradually moving from the southern part of Nanjing to the central region. The gravity center of medium high FVC was positioned in the Xuancheng area, migrating from the north of Xuancheng toward the central area and then migrating back to the northern direction of Changzhou. Finally, the gravity center of high FVC was found at the junction of Nanjing and Chuzhou, migrating from the central part of Nanjing toward Chuzhou and then migrating back to the central area. The migration direction was first to the northeast and then to the southeast.

C. FVC Change Trend and Stability Analysis

1) *Analysis of the FVC Change Trend:* The Theil-Sen median analysis and Mann-Kendall test were used to detect the change trend of FVC in the YRD from 2012 to 2021. The detection results were divided into types according to the criteria in Table III. As shown in Fig. 8, during the study period, the area of FVC improvement is slightly larger than that of FVC degradation, accounting for 49.21% and 47.51% of the total area of the YRD, respectively. The areas with significant FVC improvement trend account for 8.32% of the total area, mainly concentrate in the central and southern parts of YRD, among which Chuzhou, Hefei, Lishui, and Nanjing showed the most significant FVC

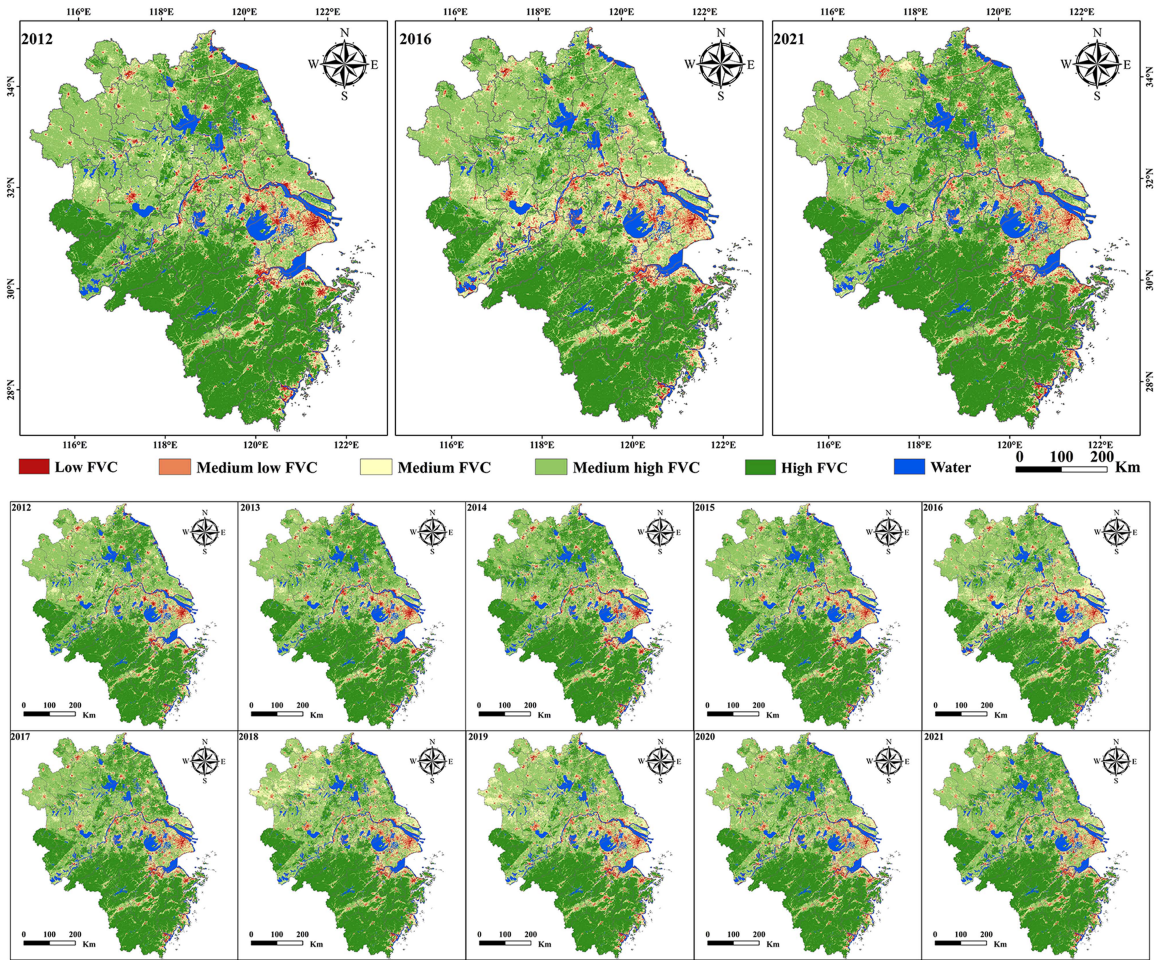


Fig. 4. Dynamic changes of FVC in the YRD from 2012 to 2021.

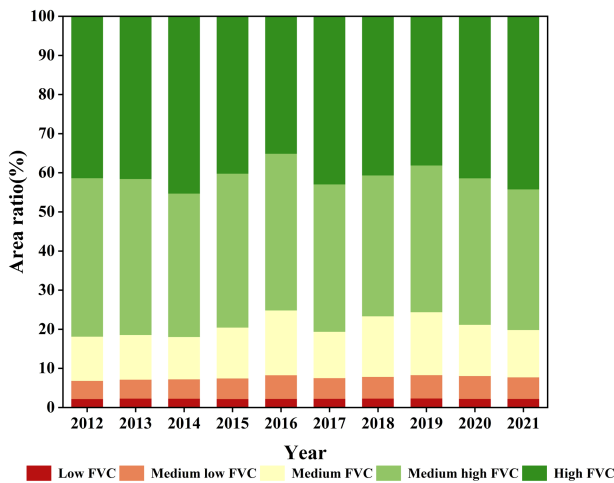


Fig. 5. Area proportion of different FVC grades in the YRD from 2012 to 2021.

improvement, accounting for 8.12%, 5.11%, 5.01%, and 4.91% of the significantly improved area, respectively.

The areas with significant FVC degradation trend account for 7.44% of the total area, mainly concentrate in the northern part of the YRD, among which Fuyang, Xuzhou, Yancheng, and Suzhou

are more obviously degraded, accounting for 9.06%, 8.62%, 6.49%, and 5.26%, respectively, of the significantly degraded area. Slightly improved and slightly degraded FVC areas are scattered throughout the study area; however, in general, they are concentrated in the southern and northern areas of the YRD, respectively.

2) *FVC Stability Analysis:* We used coefficient of variation to judge the stability of FVC in the YRD from 2012 to 2021. The detection results were divided into types according to the criteria in Table IV. The test results show (see Fig. 9) that the FVC in the YRD from 2012 to 2021 presents an overall stable local fluctuation, the southern area is stable and the central and northern fluctuation, of which the most significant fluctuation is in the area of Taihu Lake Basin (the average CV in this basin is reach 0.1464. Relatively high fluctuation grade and high fluctuation grade account for 34.11% of the basin area, far more than similar areas).

Relatively low fluctuation accounts for the largest proportion of the study area, 48.26%, basically evenly distributed in the study area. Low fluctuation is the second largest, accounting for 20.81%, mainly distributed in the study area of high FVC cover and low FVC areas. Moderate fluctuation accounts for 16.89%, mainly distributed in the middle FVC and medium high FVC areas. Finally, relatively high fluctuation and high

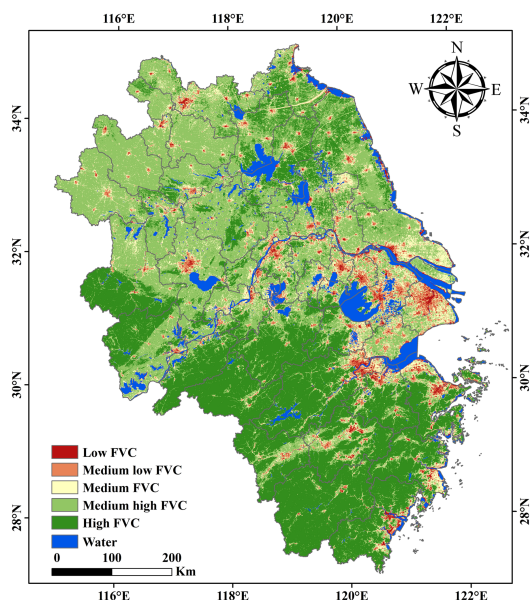


Fig. 6. Distribution of mean FVC in the YRD from 2012 to 2021.

fluctuation types account for a smaller proportion of 5.69% and 8.35%, respectively, mainly distributed in the middle and low FVC areas. Regionally, the cities with the highest fluctuations in FVC are Suzhou, Shanghai, Wuxi, Changzhou, and Jiaying, with CV averages ranging from 0.1452 to 0.1815. The cities with the lowest fluctuations in FVC are Lishui, Huangshan, Chizhou, Wenzhou, and Xuancheng, with CV averages ranging from 0.0599 to 0.0741.

D. Analysis of the Driving Mechanism of the Dynamic Change of FVC

1) *Effects of the Climate Change and Human Activity on the FVC Change:* The effects of climate and human activities on the dynamics of FVC were separated by multivariate residual regression analysis to obtain FVC_{CC} and FVC_{HA} for each year. $Slop(FVC_{CC})/slop(FVC_{HA})$ were obtained by trend analyzing them separately. They were classified according to the rules in Table V to represent the improvement or degradation of FVC under the influence of two different factors, respectively. As shown in Fig. 10, evident spatial heterogeneity exists in the influence of climate change and human activity on the developmental direction of FVC in the YRD. Overall, in the study area, regions where the climate change has a restraining effect on the FVC growth covers 27.69% of the area, primarily located in the northern and western parts. Among these, the areas particularly affected by the restraining impact of the climate change include Fuyang, Bozhou, Xuzhou, the southern parts of Lu'an, and the northern parts of Hangzhou. Areas where the climate change promotes FVC growth constitute 37.20% of the region. These areas are mainly distributed in the central-eastern and southern parts. Specifically, the promotion areas in the central-eastern region are primarily along the cities on both sides of the Yangtze River, such as Nanjing and Shanghai, whereas the southern regions mainly extend to the south of Hangzhou Bay, including cities such as Lishui and Shaoxing. Regions with relatively weak

influences of the climate change on FVC account for 35.11% and are dispersed throughout the entire YRD [see Fig. 10(a)].

Regarding changes in human activity, the areas where human activity changes restrain the FVC growth cover 39.23%, whereas the areas where human activity changes promote FVC growth cover 33.98%, with 26.79% being less affected. In comparison with the climate change, a significant increase is noted in the area where human activity restrains the growth of FVC, especially in the northern regions. In contrast, for the regions promoting the growth of FVC, there is not a significant change in the proportion of the area, it is still predominant in the central and southern parts. However, a significant increase in the concentration is noted along both sides of the Yangtze River, and there is a notable shift in the impact orientation in the western region [see Fig. 10(b)].

To further judge whether the dynamics of FVC in the same region was influenced by one factor or both factors together. We classified them into six categories according to the identification criterion for $Slop(FVC_{CC})/slop(FVC_{HA})$ in Table VI. As depicted in Fig. 11, approximately 30.83% of the YRD displays a combined effect of climate change and human activity as the driving factor for decreased FVC. In 9.37% of the area, FVC decreased are due to climate change alone and are primarily situated in the southern parts of Lu'an and northern Anqing, as well as in the northern parts of Hangzhou. Areas solely impacted by human activity causing FVC decreased cover 9.38% are mainly distributed in Huai'an, Huangshan, and Lishui. In addition, around 28.11% of the area exhibits a combined effect of the climate change and human activity as a driving factor for increased FVC. Regions solely influenced by the climate change causing FVC increased cover 7.01% and are widely dispersed, whereas areas solely influenced by human activity causing FVC increased cover 15.30%, mainly found in the southern parts of Anhui Province. In summary, during the study period, the combined influence of the climate change and human activity was identified as the primary cause of dynamic changes in FVC in the YRD.

2) *Relative Contributions of the Climate Change and Human Activity to FVC Change:* In order to quantitatively analyze the impact of climate and human activities on FVC, calculations were made with reference to the equations in Table VI. The relative contribution rate of the two factors was further obtained.

Fig. 12(a) shows that the regions in the YRD affected by the climate change resulting in a negative contribution to FVC changes constitute 64.89%. Among these, areas with a contribution of less than -20% cover 34.98% of the study area and are most concentrated in the northern parts of Anhui like Fuyang, Bozhou, Huaibei, and Suqian, and the eastern parts of Jiangsu, such as Yancheng and Nantong. Other negatively influenced areas are widespread in the central and southern parts of the YRD. Regions influenced by the climate change with a positive contribution to FVC changes account for only 35.11% of the total area. Among these, areas with a contribution exceeding 80% cover approximately 9.73% and are primarily concentrated in southern Zhejiang Province, including cities such as Ningbo, Shaoxing, and Lishui.

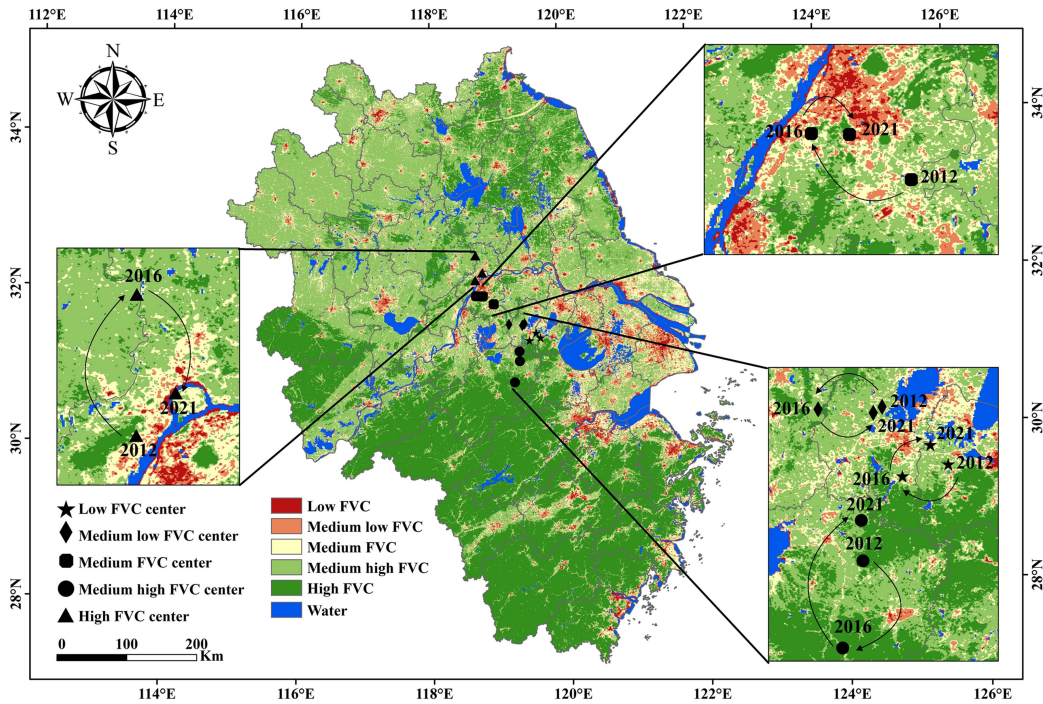


Fig. 7. Center of gravity migration of various levels of FVC in the YRD from 2012 to 2021.

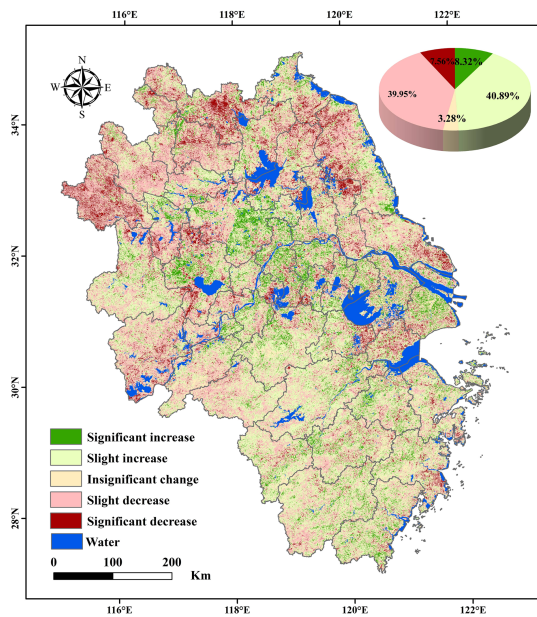


Fig. 8. Change trend of FVC in the YRD from 2012 to 2021.

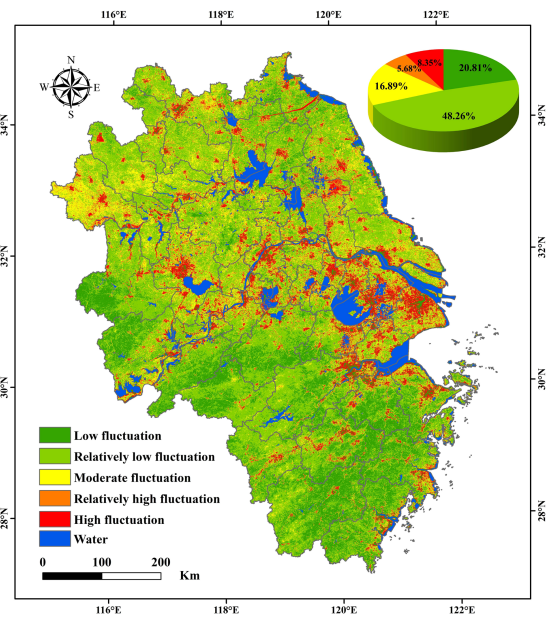


Fig. 9. Coefficient of variation of FVC in the YRD from 2012 to 2021.

Fig. 12(b) shows that the regions in the YRD affected by human activity resulting in a negative contribution to FVC changes constitute 56.59%, dominating and showing a distribution pattern similar to the areas with negative contributions from climate, particularly those below 20%. However, there is an increase in the positive contribution area, especially in the regions with a contribution greater than 80%, covering 20.64%. These are primarily distributed in the southern parts of Anhui and northern parts of Zhejiang, around the Yangtze River.

E. Resolution

1) *Effects of Various Detection Factors on the Spatial Heterogeneity of FVC:* The factor detector results, as depicted in Fig. 13, show the influence of various factors on the spatial heterogeneity of FVC ranked from high to low as follows: elevation, slope, landform type, vegetation type, soil type, night time light, precipitation, temperature, and aspect.

In terms of explanatory power, three factors-elevation, slope, and landform type-each exceed 40% in explanatory power, at

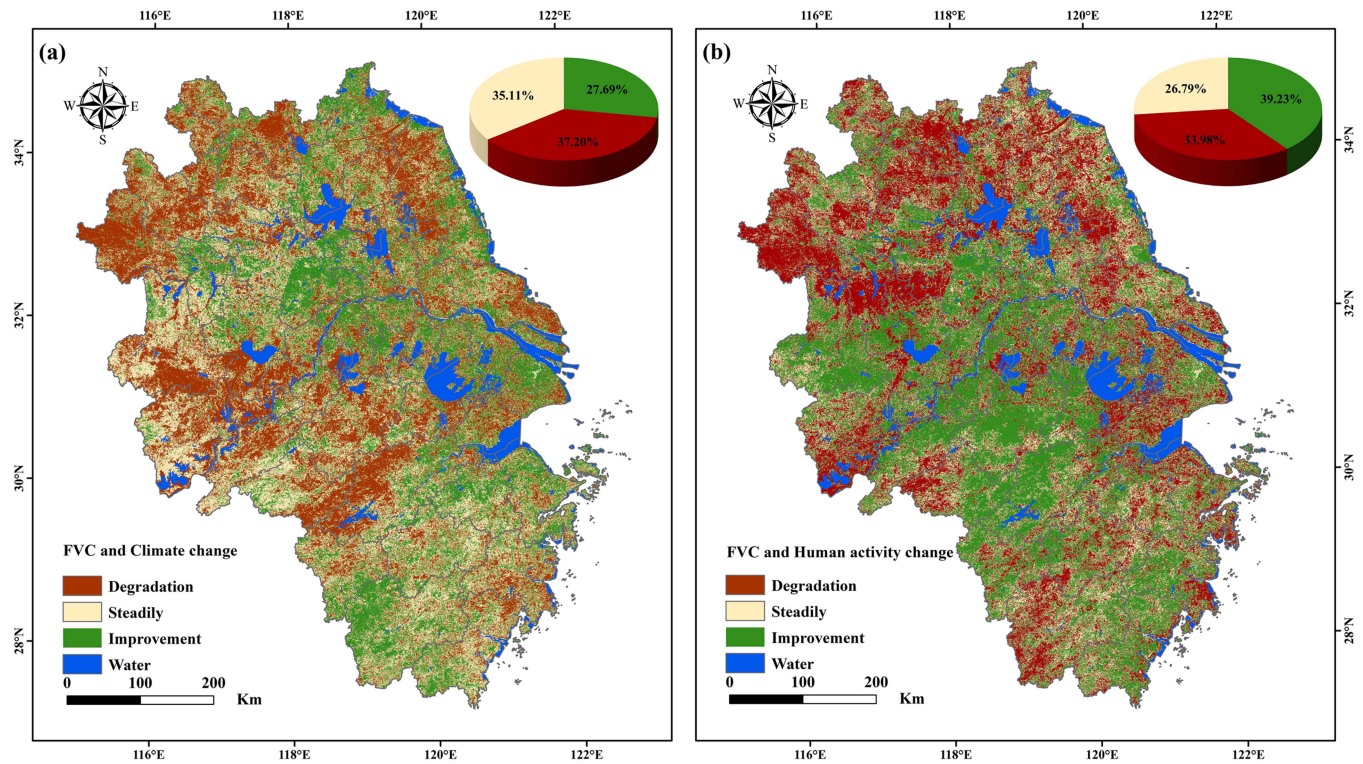


Fig. 10. Spatial distribution of the climate change effect and human activity change effect on the dynamic change of FVC in the YRD from 2012 to 2021 and (a) climate change effect on FVC and (b) human activity change effect on FVC.

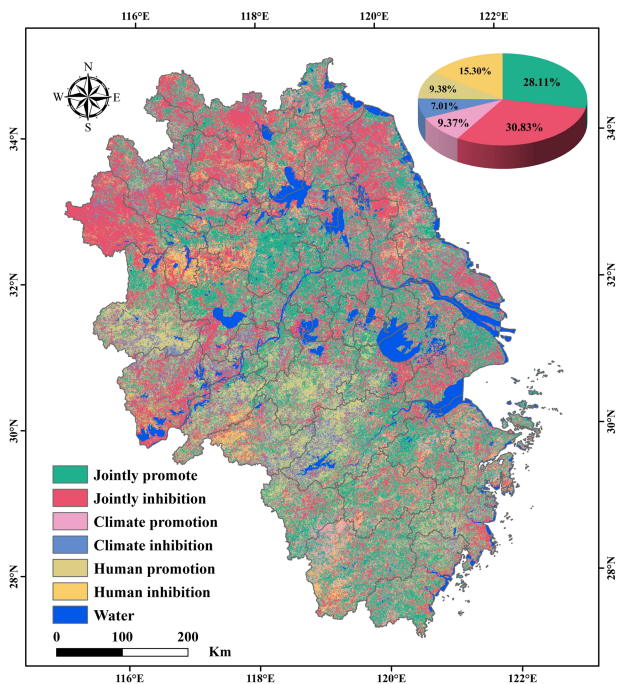


Fig. 11. Spatial distribution of driving factors of dynamic change in FVC in the YRD from 2012 to 2021.

46.85%, 45.35%, and 45.09%, respectively, establishing them as the primary factors affecting FVC in the YRD. Vegetation type, soil type, and night time light have explanatory powers between 30% and 40%, at 37.33%, 35.21%, and 32.98%, respectively,

as secondary major influencing factors. Precipitation, with an explanatory power of 29.78% falling within the 20–30% range, is a minor influencing factor. Temperature, at 6.01%, is a tertiary influencing factor. Although aspect has some impact on plant growth, it has a negligible explanatory power of only 0.09% regarding FVC in the YRD.

2) *Interaction Between Driving Factors:* In this study, the interaction detector was used to further assess the influence of interactions between various factors on the spatial heterogeneity of FVC in the YRD. The results (see Fig. 14) indicate that the interactions between various factors exhibit two types of relationships: two-factor enhancement and nonlinear enhancement. Independence or mutual weakening does not exist among the factors. This observation suggests that vegetation growth within the study area is not constrained by a single factor; however, it is the result of the synergistic effects of multiple factors. In all interaction detection results, the explanatory power of the aspect with other factors is relatively poor, consistently ranking the lowest in the combination results with various factors. Similarly, temperature consistently ranks low in combinations with the night-time light, slope, vegetation type, soil type, and other factors. The combination with the strongest explanatory power for FVC among the interaction detection results is the interaction between the primary influencing factors: elevation, slope, landform type, and night-time light, explaining more than 60% of the explanatory power. Furthermore, the interactions of other factors with elevation, landform type, and slope consistently rank in the top three to four positions in terms of explanatory power. The color gradient in the graph indicates that interactions

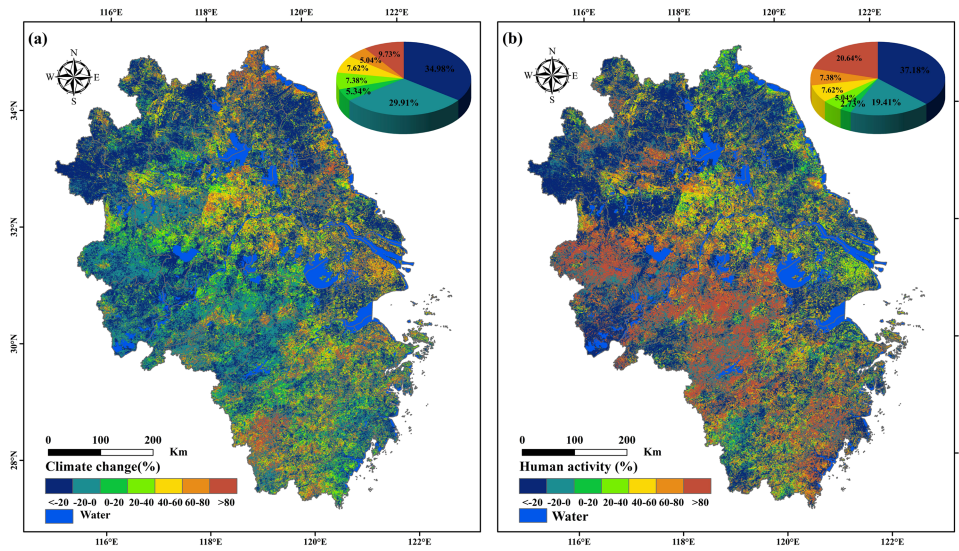


Fig. 12. Spatial distribution of relative contributions of the climate change and human activity to FVC in the YRD from 2012 to 2021 and (a) relative contribution of the climate change to FVC and (b) the relative contribution of human activity to FVC.

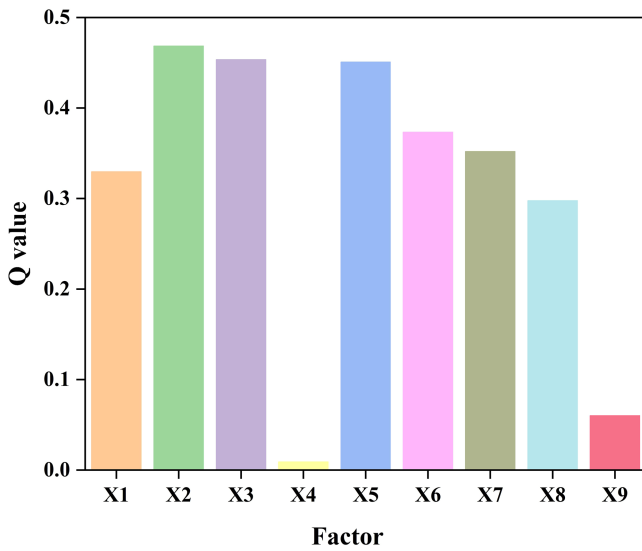


Fig. 13. Influence factor q value spatial heterogeneity of FVC in the YRD.

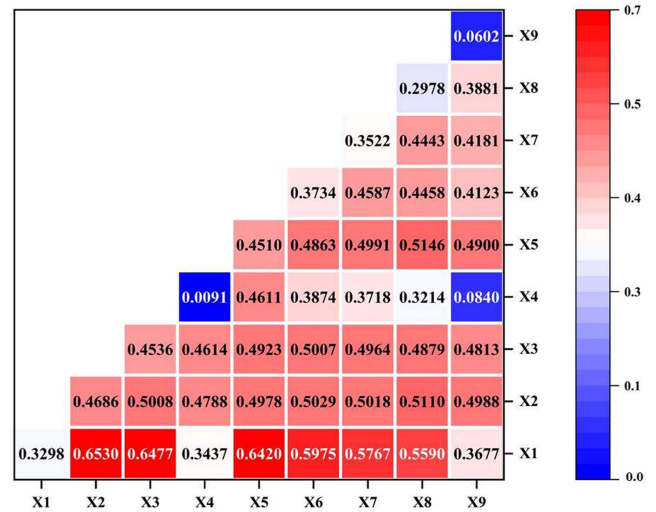


Fig. 14. Interpretation of the detection factor interaction.

with explanatory power above 54% predominantly occur within combinations involving the night-time light. The explanatory power of night-time light is significantly enhanced in combination with other high-explanatory-power factors, emerging as the most dominant influencing factor in the study area. These results further support the conclusion drawn from the factor detector analysis, emphasizing that temperature and slope have weaker impacts on FVC within the study area compared to elevation, aspect, and the landform type, which exhibit stronger influences.

3) *Range or Type of Adaptation of the Driver Factors to FVC:* Using the risk detector, the suitability of vegetation in various types or ranges of each factor for survival was explored. A higher FVC value indicates greater suitability of that factor’s characteristics for vegetation growth.

As depicted in Fig. 15, FVC shows higher suitability for FVC when night-time light below $<3.6 \text{ nW/cm}^2/\text{sr}$ and exhibits the poorest suitability in the range of $29.6\text{--}63.7 \text{ nW/cm}^2/\text{sr}$. During risk detection of night-time light, as the grades increase, FVC values show a sharp decline. Notably, during detection of the fourth and fifth grades, FVC suitability drops below 20%. Apart from grassland in vegetation types, FVC ranks the lowest among the suitability grades for various factors. The reason is human intervention, which affects the natural state of surface vegetation, consequently leading to a continuous decline in its survival suitability.

When the elevation is in the range 533–692 m, it is more suitable for the survival of FVC, whereas it is less suitable when the elevation is less than 54 m. Regarding the landform type, FVC is most suitable in mountainous areas, whereas its suitability is less

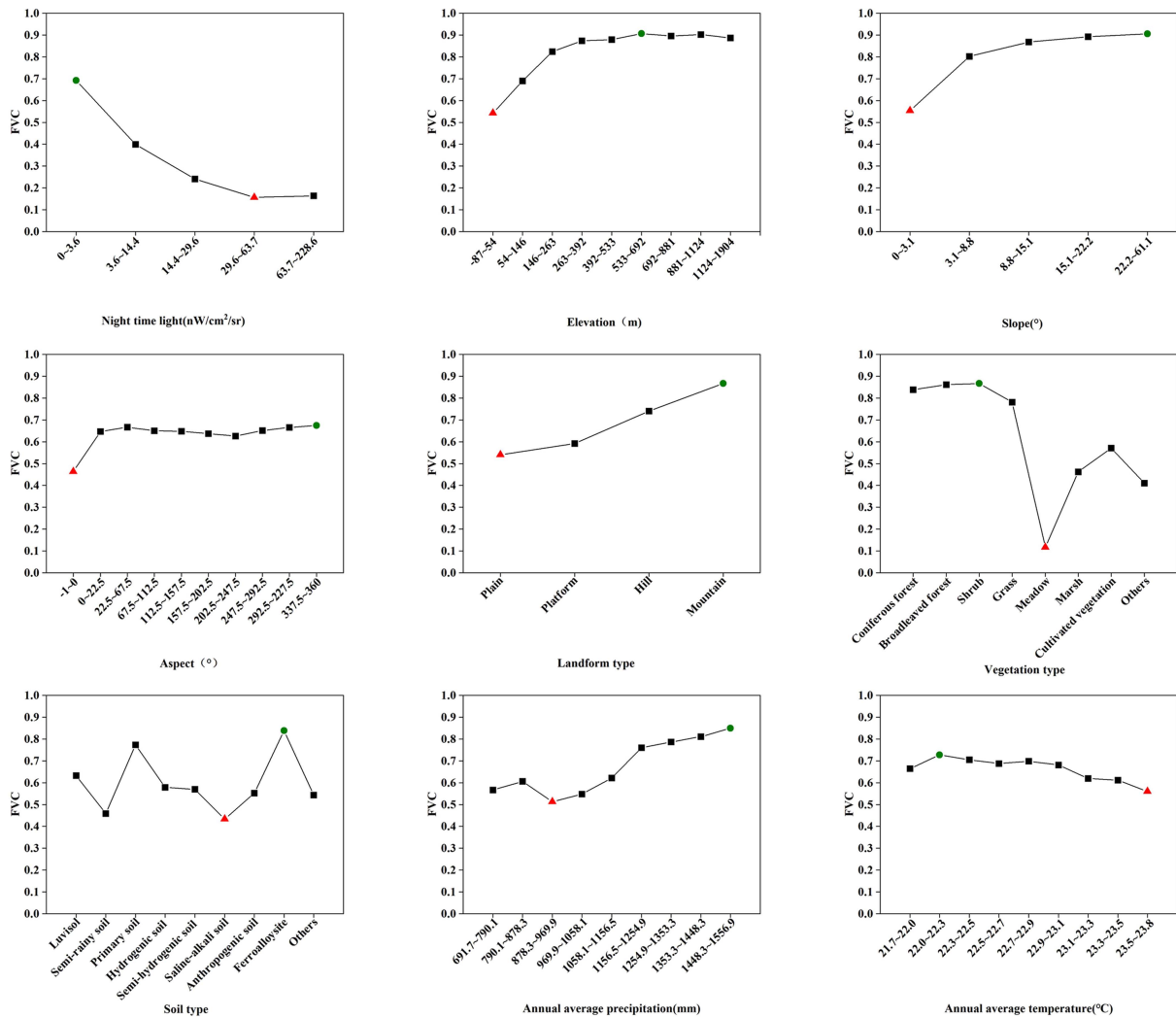


Fig. 15. Suitable range of each factor index in the YRD.

favorable in plains. Regarding elevation detection, the suitability trend for FVC shows an initial increase followed by a gradual decrease. As elevation increases, the impact of human activities weakens and there is abundant rainfall, creating favorable conditions for vegetation growth. However, when the elevation reaches the range of 533–692 m, the increase in height leads to reduced precipitation and inadequate thermal conditions, instead limiting the vegetation growth instead.

During the investigation of the slope factor, as slope steepness increased, the suitability for FVC continually improved. The variation in slope grades plays a role in filtering vegetation types in the YRD. At lower slope grades, cultivated vegetation and grasslands are more prevalent, whereas at higher grades, broad-leaved forests, coniferous forests, and shrubs dominate. Considering the results of vegetation types, the FVC values are highest under broad-leaved forests, coniferous forests, and shrub types, whereas grasslands, marshes, cultivated vegetation, and grasslands generally exhibit lower FVC values than arboreal vegetation. Therefore, an increase in the slope steepness concurrently enhances the FVC adaptability. YRD is dominated by a subtropical monsoon climate. High temperatures in summers

lead to severe water loss. With increased frequency of extreme climates and global warming, vegetation demands for water gradually increased. Based on the suitability detection results for precipitation, precipitation grades of 878.3–969.9 mm and below may not adequately meet the requirements for vegetation growth. However, beyond this range, as the precipitation increases, FVC suitability rapidly increases. In terms of acquiring heat, temperatures of 22.0–22.3°C and below can essentially meet the demands for vegetation growth. Excessive heat can cause chlorophyll deactivation, reducing the rate of photosynthesis, accelerating evaporation of water within plants, causing dehydration, and reducing vegetation survival capability. Hence, subsequent temperature grades show a decreasing trend in vegetation suitability.

Although this aspect has a weak impact on the spatial variation of FVC within the study area, certain differences in the suitability of FVC still exist at various grades. Among these, the highest suitability is observed for the north, northeast, and northwest aspects. In the YRD, the mountain ranges mainly run from the northeast to southwest direction, with the northern slopes essentially acting as windward slopes. Compared with leeward

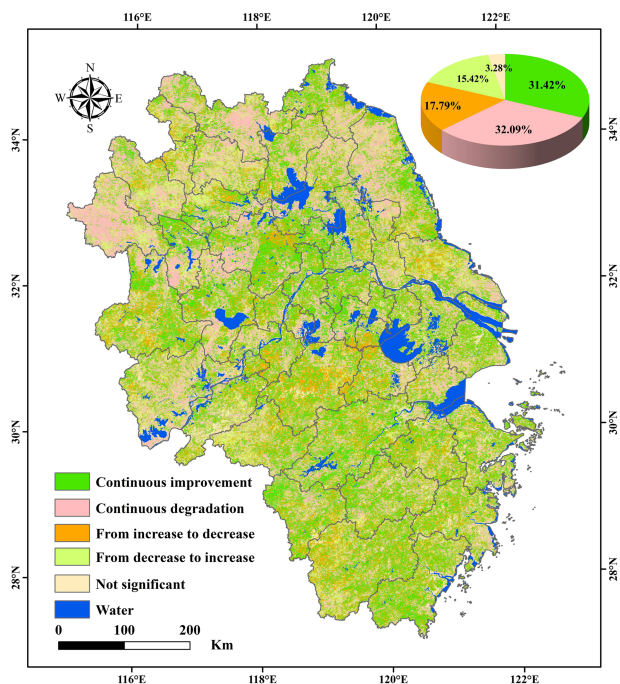


Fig. 16. Future development trend of FVC in the YRD.

slopes, windward slopes receive more abundant precipitation, which is more conducive to vegetation growth.

In the study area, various soil types exhibit varying effects on FVC suitability. Ferroalloy soils are primarily located in mountainous regions, and their suitability for FVC is influenced to a certain extent by factors such as elevation and landform. Conversely, saline-alkali soils negatively impact the vegetation growth.

F. Future Development Trends of the FVC

The Hurst index for FVC in the YRD ranges from 0.06 to 0.99, with an average of 0.55. Regions with a Hurst index >0.5 account for 63.96%, indicating dominance, whereas those with <0.5 account for only 33.21%. This difference indicates the sustainability of FVC development in the YRD; most areas in the study region are likely to continue their current trends in the future. To further understand the future development trend of FVC in the study area, the Hurst index was coupled with the trend test results obtained earlier for analyzing the development of future FVC in the YRD (see Fig. 16).

The results are divided into five categories: regions showing continuous improvement and degradation account for the largest proportions, at 31.42% and 32.09%, and are respectively, widely distributed across the entire region. Areas showing continuous improvement are mainly concentrated in the central part of the YRD, including Chuzhou, Nanjing, Ma'anshan, Zhenjiang, and most mountainous areas in the southern part of Zhejiang Province.

Conversely, areas exhibiting continuous degradation are primarily located in the northern border cities of the YRD, such as Fuyang, Xuzhou, and Yancheng. Regions transitioning from growth to degradation occupy 17.79% and are predominantly

concentrated in the south of Xuancheng, Wuhu, southern Wuxi, and western Huzhou. Meanwhile, areas transitioning from degradation to growth cover 15.42%, primarily focused around the convergence of Bengbu, Bozhou, and Suzhou, with some relatively dense concentrations in the western part of Huangshan City.

IV. DISCUSSION

A. Discussion on the Spatiotemporal Dynamics of FVC in the YRD

From 2012 to 2021, the overall FVC in the YRD showed a nonsignificant decreasing trend, with noticeable spatial heterogeneity. Before 2016, a rapid decline in FVC was observed, followed by a fluctuating increase after 2016. The northern part of the study area, characterized by a flat terrain and the period when the rainy season and hot season occur simultaneously is conducive to cultivating vegetation, with a dominance of medium highly FVC. In contrast, the southern regions, which are rich in mountainous terrain, are favorable for forest growth, exhibiting a concentration of high FVC. These findings align with the results of Yuan et al. [53].

The increase in the frequency and intensity of extreme climatic events led to frequent natural disasters, significantly affecting the vegetation growth [54], [55], [56]. We believe this will cause some short-term decline in vegetation, followed by a gradual recovery. As depicted in Fig. 2, turning points in FVC change occurred in 2013, 2016, and 2019. According to Yuan et al. [53], the temporal lag in the response of NDVI in the YRD to temperature is nearly nonexistent. In 2013, during summers, the subtropical high-pressure system in the YRD was exceptionally strong, resulting in a shorter rainy season and severe drought in the middle and lower reaches of the Yangtze River, leading to a decrease in vegetation cover. Natural disasters such as floods, landslides, and debris flows can cause rapid declines in FVC due to significant erosion and loss of vegetation in the short term [20]. In 2016, intense rainfall occurred in the middle and lower reaches of the Yangtze River [57], causing serious damage in Jiangsu, Zhejiang, and Anhui provinces, resulting in a significant decrease in FVC that year. The noticeable decline in vegetation in 2019 may have been influenced by El Niño, causing alternating droughts and floods, weakening the growth capabilities of the vegetation [58].

However, for the emergence of turning trends in longer time series, we believe that they should be analyzed by Stage data. As can be seen in Fig. 4, in the two phases of “2012–2016 and 2016–2021,” the regions with the most significant changes in FVC are mainly concentrated in the central region, with the changes on both sides of the Yangtze River being particularly prominent. Therefore, we mainly analyze this region. According to Fig. 11, the dynamics of FVC in the YRD region is mainly driven by both climate and human activities. Therefore, we will analyze these two aspects. In order to show the impacts of these two factors at different stages more intuitively, we have conducted the mean processing of FVC_{CC} and FVC_{HA} in “2012–2016 and 2016–2021,” respectively (to remove the influence of the original vegetation base, the mean value of FVC

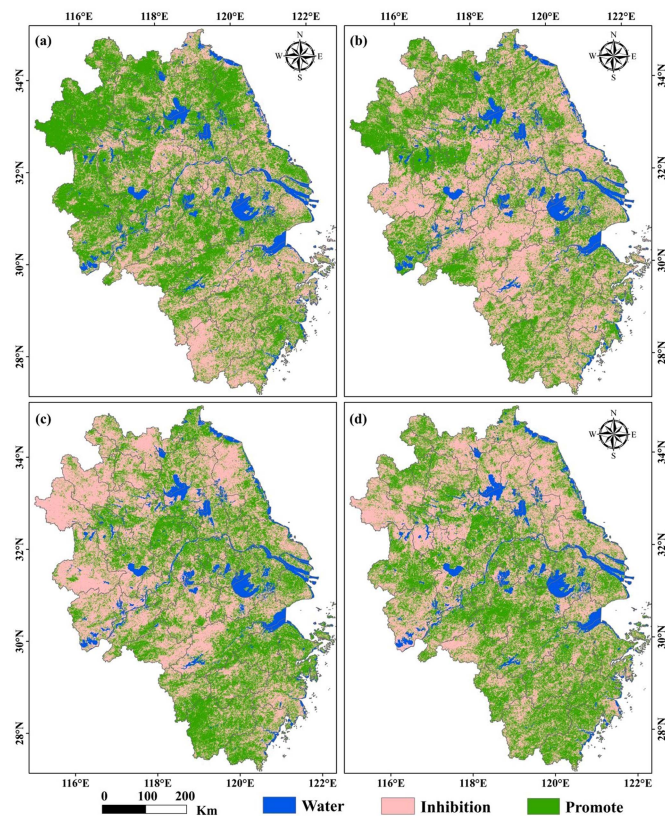


Fig. 17. Positive and negative impacts of climate change and anthropogenic changes on FVC in the YRD and (a), (b) 2012–2016 climate change, anthropogenic impacts on FVC and (c), (d) 2016–2021 climate change, anthropogenic impacts on FVC.

was uniformly subtracted from FVC_{CC}). The results are shown in Fig. 17.

Comparing Fig. 17(a) and (c), we find that climate factors show opposite effects in the two phases for the specified regions. It shows: Midwest promote, Mideast inhibition–Midwest inhibition, Mideast promote. By analyzing the meteorological data of the relevant years, we found that the temperature did not change much but precipitation increased and then decreased during the two phases in the Midwest region. Fig. 15 shows that the increase in precipitation contributes to the survival suitability of FVC. In the central and eastern regions, precipitation did not change strongly, but the temperature in the first stage was below 22°C, while the temperature in the second stage was 22–23°C, which increased the survival suitability of FVC. Combined with Fig. 17(b) and (d), we find that the results of human activities in these two phases are strongly contrasting, with an “inhibition–promote” shift. We believe that this is mainly due to the positive effect of a series of related policies, such as the “Outline for the Development of China’s Ecological Civilisation (2016–2020).”

Combined with the above analyses, we believe that the impacts of human activities are more focused and prominent, ultimately leading to a long time-series transition.

Further analysis of FVC change trends in various prefecture-level cities revealed that Fuyang and Xuzhou experienced the most severe degradation in FVC during the study period. Combining the research findings on the dynamic changes in FVC,

this study indicates that the FVCs of both cities is significantly negatively affected by climatic and human activities, leading to a pronounced degradation trend. These results align with those of Zhao et al. [59]. In terms of climate, Fuyang, located south of the Huai River, experiences a transitional climate characterized by a gradual shift from temperate monsoons to subtropical monsoons. This caused it to have disadvantages of both northern and southern climates. During some years, there is little rainfall leading to drought, whereas in other years, there is heavy rainfall causing floods. The region frequently experiences droughts and floods, demonstrating a significant climatic variability [60]. Regarding human activities, this can be related to extensive cutting of poplar trees in the region. In recent years, Fuyang has drastically reduced the area of poplar tree plantations, from nearly 2 million mu (Chinese measurement) to about 600,000 mu, in response to the poplar fluff affecting local residents [61]. Therefore, there is a significant negative impact between human activities and FVC in this area, and the results are basically consistent with the analysis of the impact of human activities in Fuyang by Zhao et al. [59]. Although comprehensive afforestation measures were later implemented, to intensify nursery cultivation and afforestation efforts, the lengthy process of vegetation recovery still resulted in a significant degradation trend. Xuzhou shares similar climate with Fuyang, thus exhibiting a strong negative climate–vegetation relationship. The negative impact driven by human activities in Xuzhou can be attributed to the developed industrial and mining activities in the region, leading to substantial subsidence from coal mining and inadequate vegetation protection, resulting in severe dust pollution [62], [63]. These conditions indicate that this region lacks tall arbor-type vegetation, as tall arbors can help mitigate dust pollution by acting as windbreakers.

During the study period, the provincial capital cities, Hefei in Anhui and Nanjing in Jiangsu, were among the leaders in improving vegetation. As shown in Fig. 8, significant improvements in FVC were observed in the core area of Shanghai along both banks of the Huangpu River, as well as in the northern region of Hangzhou. These areas are all part of their respective provincial or municipal cores. Considering Shanghai as the most representative case for analyzing the underlying reasons for vegetation improvement, it was observed that during the study period, both climate and human activities had a positive impact on the FVC in the core area of Shanghai. Shanghai now focuses on ecological environmental protection and progress. This city shifted from reducing pollutant emissions to improving environmental quality and enhancing ecological service functions. As of the end of 2021, the forest cover reached 19.4% and the per capita public park green area reached 8.8 square meters [64]. In contrast, the subtropical monsoon climate and proximity of this city to the ocean, with abundant moisture, along with suitable temperatures, contribute to favorable conditions for vegetation growth.

On comprehensive analysis of FVC change trends and fluctuations, it was observed that both areas with insignificant vegetation changes and those with small fluctuations dominate in the YRD. This is primarily because of two reasons. First, in the YRD, cultivated plants are one of the dominant vegetation

types, mainly on arable land. However, because of China's strict protection policies for arable land [65], the changes in planting area and density are relatively small. Second, in most parts of the Zhejiang Province and the Dabie Mountains in Anhui, forests are the dominant vegetation. The rugged terrain not only provides favorable hydrothermal conditions but also reduces human interference, contributing to relatively stable vegetation growth. This observation aligns closely with the findings of Liu et al. [17].

B. Multipart Figures

1) *Driving Mechanism of the FVC Dynamic Change*: During the study period, the combined effects of climate and human activities emerged as the primary driving forces behind both the improvement and degradation of FVC in most areas of the YRD.

In the northern regions of the study area, FVC is predominantly influenced by the joint inhibitory impact of climate and human activities. These areas are mostly situated within the Huai River basin, which is characterized by a transition from a temperate monsoon to a subtropical monsoon climate, leading to frequent droughts and floods [60]. Recent warming temperatures and an increase in extreme rainfall events have worsened these disasters [66]. The Huai River basin is one of the China's major grain-producing areas with extensive farmland, primarily consisting of cultivated vegetation. Frequent meteorological disasters caused significant losses in agricultural production [67], further hindering the growth of FVC. On the other hand, as discussed earlier regarding the causes of FVC degradation in cities like Fuyang and Xuzhou, some government decisions related to vegetation and the degradation of vegetation caused by local economic development are also reasons for restraining the growth of FVC. The combined promotion of FVC by climate and human activities is predominantly observed in the central and southern regions of the study area. These regions experience higher precipitation than the northern parts, providing more favorable conditions for vegetation survival. However, excessive rainfall can diminish the absorption of heat by the vegetation and slow down the decomposition of organic matter and nutrient release in the soil [29]. Yet, the warming temperatures partly counteract this issue, enabling climate change to promote FVC. In terms of human activities, more scientific measures are taken while pursuing the idea that "green mountains and clear water are invaluable assets," thereby balancing economic development with environmental conservation.

2) *Driving Mechanism of FVC Spatial Heterogeneity*: Based on the findings of the factor detector, it is evident that the spatial heterogeneity of FVC within the study area is influenced by both natural and human activity factors. The results from interaction detection indicate a significant enhancement in the explanatory power of combined factors compared with that of single factors. This observation signifies that the spatial heterogeneity of FVC is primarily shaped by interacting composite factors. Notably, the high concentration of interaction explanatory power demonstrates that the explanatory power of human activity factors significantly increases when combined with the natural factors, aligning with findings of Kolluru [68].

3) *Limitations and Deficits*: This study employed NDVI to estimate FVC. However, in areas where FVC exceeds 85%, NDVI becomes less sensitive to changes [69], leading to reduced inversion accuracy. Future research will attempt to use more effective vegetation indices for FVC estimation. In exploring the dynamic mechanisms of FVC changes, only the climatic data were analyzed according to the annual average temperature and precipitation data, leaving room for improvement in comprehensiveness. Despite the current research indicating that precipitation and temperature are the main factors that influence vegetation changes in the YRD [32], [53], other climate factors such as solar radiation, atmospheric humidity, and sunshine duration may also affect vegetation. Future studies will incorporate more climatic elements for further analysis. Regarding the analysis of spatial heterogeneity of FVC, night-time light was chosen to represent the human activity factor. This dataset has widespread applications in assessing urban expansion, economic activities, and estimating population density, serving as a powerful tool for modeling socioeconomic indicators [70], [71]. Substituting night-time remote sensing data for purely regional economic and population indicators can enhance the accuracy of detection results. However, the impact of ideological changes in human activity were ignored in the research process. Future research will further introduce data on the number of universities in various regions and the proportion of technological investment to refine the entire detection system.

V. CONCLUSION

This article focuses on the YRD and conducts a study based on MODIS NDVI data to explore the temporal and spatial variation characteristics and driving force mechanism of FVC from 2012 to 2021. The main conclusions of this study are as follows:

- 1) The FVC variation in the YRD from 2012 to 2021 can be divided into two phases: a rapid decline before 2016 followed by fluctuating increases after 2016, remaining within the range of 0.61–0.67. The average FVC exhibited strong spatial heterogeneity with a pattern of higher values in the west, lower values in the east, higher values in the north and south, and lower values in the central part. High and medium high FVCs dominated the study area. Notably, there was a noticeable shift in the centroid of various FVC grades during the study period, with a tendency of regression from west to east observed in all cover grades except for high FVC. The FVC in the YRD showed overall development tending toward stability, but the fluctuation was more pronounced in the Taihu Lake Basin. Improvement areas were mainly concentrated on both sides of the Yangtze River in the central part of the YRD and in the southern mountainous region. Degraded areas were concentrated in cities north of the Huai River.
- 2) The changes in FVC in most parts of the YRD were driven by both dynamic factors: climate and human activities. FVC in the northern region was mainly restrained by climate and human activities, whereas in the central and southern regions, FVC was primarily driven by the combined promotion of these factors.

- 3) Natural factors exhibited relatively stronger explanatory power for spatial differentiation than human activity. The order of influence of various factors on the distribution of FVC in the YRD was as follows: elevation, slope, landform type, vegetation type, soil type, night-time light, precipitation, temperature, and aspect. After interactions between factors, there was an enhancement in the explanatory power. Notably, the combination of human activity factors significantly increased the explanatory power when combined with natural factors, with the most influential combination being elevation \cap night-time light, exhibiting an explanatory power of 0.6530.
- 4) The development of FVC in the YRD is sustainable. Most areas within the study region are expected to maintain the current trend in the future, continuing the existing patterns of improvement in the central and southern parts and degradation in the northern parts.

This study has advanced our understanding of the characteristics and driving mechanisms of FVC changes in economically developed regions like the YRD in China. The research findings can serve as a scientific basis for the protection and restoration of the ecological environment in the YRD.

ACKNOWLEDGMENT

The authors thank the Editor and the anonymous reviewers for their valuable comments, which have led to further improvements in the quality of this manuscript.

REFERENCES

- [1] W. Rina et al., "Multi-climate factors and the preceding growth stage of vegetation co-regulated the variation of the end of growing season in northeast inner Mongolia, China," *IEEE Access*, vol. 8, pp. 221525–221538, 2020.
- [2] Y. Cai, M. Zhang, and H. Lin, "Estimating the urban fractional vegetation cover using an object-based mixture analysis method and Sentinel-2 MSI imagery," *IEEE J. Sel. Topics Appl. Earth Observ. Remote Sens.*, vol. 13, pp. 341–350, 2020.
- [3] K. Jia et al., "Global land surface fractional vegetation cover estimation using general regression neural networks from MODIS surface reflectance," *IEEE Trans. Geosci. Remote Sens.*, vol. 53, no. 9, pp. 4787–4796, Sep. 2015.
- [4] A. Daham, D. Han, M. Rico-Ramirez, and A. Marsh, "Analysis of NVDI variability in response to precipitation and air temperature in different regions of Iraq, using MODIS vegetation indices," *Environ. Earth Sci.*, vol. 77, pp. 1–24, 2018.
- [5] J. Wang, K. Wang, M. Zhang, and C. Zhang, "Impacts of climate change and human activities on vegetation cover in hilly southern China," *Ecological Eng.*, vol. 81, pp. 451–461, 2015.
- [6] Y. Liu, Y. Li, S. Li, and S. Motesharrei, "Spatial and temporal patterns of global NDVI trends: Correlations with climate and human factors," *Remote Sens.*, vol. 7, no. 10, pp. 13233–13250, 2015.
- [7] Z. Ma, J. Guo, W. Li, Z. Cai, and S. Cao, "Regional differences in the factors that affect vegetation cover in China," *Land Degradation Develop.*, vol. 32, no. 5, pp. 1961–1969, 2021.
- [8] W. Jiang, L. Yuan, W. Wang, R. Cao, Y. Zhang, and W. Shen, "Spatio-temporal analysis of vegetation variation in the Yellow River Basin," *Ecological Indicators*, vol. 51, pp. 117–126, 2015.
- [9] L. Jiang, A. Bao, H. Guo, and F. Ndayisaba, "Vegetation dynamics and responses to climate change and human activities in Central Asia," *Sci. Total Environ.*, vol. 599, pp. 967–980, 2017.
- [10] L. Ma, Y. Zhou, J. Chen, X. Cao, and X. Chen, "Estimation of fractional vegetation cover in semiarid areas by integrating endmember reflectance purification into nonlinear spectral mixture analysis," *IEEE Geosci. Remote Sens. Lett.*, vol. 12, no. 6, pp. 1175–1179, Jun. 2015.
- [11] H. Jiang et al., "Angular effect correction for improved LAI and FVC retrieval using GF-1 wide field view data," *IEEE Trans. Geosci. Remote Sens.*, vol. 61, 2023, Art. no. 4407414.
- [12] S. Wu et al., "Approach for monitoring spatiotemporal changes in fractional vegetation cover through unmanned aerial system-guided-satellite survey: A case study in mining area," *IEEE J. Sel. Topics Appl. Earth Observ. Remote Sens.*, vol. 16, pp. 5502–5513, 2023.
- [13] A. Bannari, D. Morin, F. Bonn, and A. Huete, "A review of vegetation indices," *Remote Sens. Rev.*, vol. 13, no. 1–2, pp. 95–120, 1995.
- [14] W. Zhou, C. Gang, J. Li, C. Zhang, S. Mu, and Z. Sun, "Spatial-temporal dynamics of grassland coverage and its response to climate change in China during 1982–2010," *Acta Geographica Sinica*, vol. 69, no. 1, pp. 15–30, 2014.
- [15] Z. Zhi et al., "Spatial-temporal changes of vegetation restoration in Yan'an based on MODIS NDVI and landsat NDVI," in *Proc. IEEE Int. Conf. Signal, Inf. Data Process.*, 2019, pp. 1–5.
- [16] M. Li et al., "Climate change and anthropogenic activity co-driven vegetation coverage increase in the three-north shelter forest region of China," *Remote Sens.*, vol. 15, no. 6, 2023, Art. no. 1509.
- [17] H. Liu et al., "Spatiotemporal evolution of fractional vegetation cover and its response to climate change based on MODIS data in the subtropical region of China," *Remote Sens.*, vol. 13, no. 5, 2021, Art. no. 913.
- [18] J. Yuan, Z. Bian, Q. Yan, Z. Gu, and H. Yu, "An approach to the temporal and spatial characteristics of vegetation in the growing season in Western China," *Remote Sens.*, vol. 12, no. 6, 2020, Art. no. 945.
- [19] R. Yang, X. Li, D. Mao, Z. Wang, Y. Tian, and Y. Dong, "Examining fractional vegetation cover dynamics in response to climate from 1982 to 2015 in the Amur river basin for SDG 13," *Sustainability*, vol. 12, no. 14, 2020, Art. no. 5866.
- [20] R. Wu, Y. Wang, B. Liu, and X. Li, "Spatial-temporal changes of NDVI in the three northeast provinces and its dual response to climate change and human activities," *Front. Environ. Sci.*, vol. 10, 2022, Art. no. 974988.
- [21] Y. Yan et al., "Exploring and attributing change to fractional vegetation coverage in the middle and lower reaches of Hanjiang River Basin, China," *Environ. Monit. Assessment*, vol. 195, no. 1, 2023, Art. no. 131.
- [22] X. Ma et al., "A pixel dichotomy coupled linear kernel-driven model for estimating fractional vegetation cover in arid areas from high-spatial-resolution images," *IEEE Trans. Geosci. Remote Sens.*, vol. 61, 2023, Art. no. 4406015.
- [23] J. Wu, Y. Zhou, H. Wang, X. Wang, and J. Wang, "Assessing the causal effects of climate change on vegetation dynamics in Northeast China using convergence cross-mapping," *IEEE Access*, vol. 11, pp. 115367–115379, 2023.
- [24] B. Fu et al., "Evaluation of spatio-temporal variations of FVC and its relationship with climate change using GEE and Landsat images in Ganjiang River Basin," *Geocarto Int.*, vol. 37, no. 26, pp. 13658–13688, 2022.
- [25] X. Jia, G. You, S. McKenzie, C. Zou, J. Gao, and A. Wang, "Inter-annual variations of vegetation dynamics to climate change in ordos, Inner Mongolia, China," *PLoS One*, vol. 17, no. 11, 2022, Art. no. e0264263.
- [26] S. Piao et al., "Interannual variations of monthly and seasonal normalized difference vegetation index (NDVI) in China from 1982 to 1999," *J. Geophysical Res., Atmospheres*, vol. 108, no. D14, 2003.
- [27] J. Sun et al., "Optimizing grazing exclusion practices to achieve Goal 15 of the sustainable development goals in the Tibetan Plateau," *Sci. Bull.*, vol. 66, no. 15, pp. 1493–1496, 2021.
- [28] X. Li, Z. Zhang, and A. Sun, "Study on the spatial-temporal evolution and influence factors of vegetation coverage in the Yellow River Basin during 1982–2021," *J. Earth Environ.*, vol. 13, no. 4, pp. 428–436, 2022.
- [29] J. Lai, T. Zhao, and S. Qi, "Spatiotemporal variation in vegetation and its driving mechanisms in the southwest alpine canyon area of China," *Forests*, vol. 14, no. 12, 2023, Art. no. 2357.
- [30] D. Feng, J. Wang, M. Fu, G. Liu, M. Zhang, and R. Tang, "Spatiotemporal variation and influencing factors of vegetation cover in the ecologically fragile areas of China from 2000 to 2015: A case study in Shaanxi Province," *Environ. Sci. Pollut. Res.*, vol. 26, pp. 28977–28992, 2019.
- [31] L. Cui, L. Wang, R. P. Singh, Z. Lai, L. Jiang, and R. Yao, "Association analysis between spatiotemporal variation of vegetation greenness and precipitation/temperature in the Yangtze River Basin (China)," *Environ. Sci. Pollut. Res.*, vol. 25, pp. 21867–21878, 2018.
- [32] Y. Wang and D. Liang, "Temporal and spatial variation characteristics of vegetation cover and climate response in the Yangtze River Delta," *J. Anhui Normal Univ. (Natural Sci.)*, vol. 45, no. 5, 2022, Art. no. 7.

- [33] Y. Xu, Q.-Y. Dai, B. Zou, M. Xu, and Y.-X. Feng, "Tracing climatic and human disturbance in diverse vegetation zones in China: Over 20 years of NDVI observations," *Ecological Indicators*, vol. 156, 2023, Art. no. 111170.
- [34] J. Han, X. Zhang, J. Wang, and J. Zhai, "Geographic exploration of the driving forces of the NDVI spatial differentiation in the Upper Yellow River Basin from 2000 to 2020," *Sustainability*, vol. 15, no. 3, 2023, Art. no. 1922.
- [35] Y. Zuo, Y. Li, K. He, and Y. Wen, "Temporal and spatial variation characteristics of vegetation coverage and quantitative analysis of its potential driving forces in the Qilian Mountains, China, 2000–2020," *Ecological Indicators*, vol. 143, 2022, Art. no. 109429.
- [36] J. Han et al., "Driving factors of desertification in Qaidam Basin, China: An 18-year analysis using the geographic detector model," *Ecological Indicators*, vol. 124, 2021, Art. no. 107404.
- [37] A. Pan, K. Wang, Y. Zeng, Z. Xie, and Q. Miao, "Trends of temperature and precipitation variation in the Yangtze River Delta from 1961 to 2006," *Trans. Atmospheric Sci.*, vol. 34, no. 2, pp. 180–188, 2011.
- [38] Q. Ge, X. Guo, J. Zheng, and Z. Hao, "Meiyu in the middle and lower reaches of the Yangtze River since 1736," *Chin. Sci. Bull.*, vol. 53, no. 1, pp. 107–114, 2008.
- [39] J. Shi, L. Cui, and W. Zhou, "Change trend of climatic factors in the Yangtze River Delta from 1959 to 2005," *Resour. Sci.*, vol. 30, pp. 1803–1810, 2008.
- [40] B. N. Holben, "Characteristics of maximum-value composite images from temporal AVHRR data," *Int. J. Remote Sens.*, vol. 7, no. 11, pp. 1417–1434, 1986.
- [41] K. Wu and X. Wang, "Aligning pixel values of DMSP and VIIRS nighttime light images to evaluate urban dynamics," *Remote Sens.*, vol. 11, no. 12, 2019, Art. no. 14623.
- [42] Z. Gong, S. Zhao, and J. Gu, "Correlation analysis between vegetation coverage and climate drought conditions in North China during 2001–2013," *J. Geographical Sci.*, vol. 27, pp. 143–160, 2017.
- [43] X. Li, H. Zulkar, D. Wang, T. Zhao, and W. Xu, "Changes in vegetation coverage and migration characteristics of center of gravity in the arid desert region of northwest China in 30 recent years," *Land*, vol. 11, no. 10, 2022, Art. no. 1688.
- [44] M. Gocic and S. Trajkovic, "Analysis of changes in meteorological variables using Mann-Kendall and Sen's slope estimator statistical tests in Serbia," *Glob. Planet. Change*, vol. 100, pp. 172–182, 2013.
- [45] T. Carvalho, A. A. S. Jorge, T. Bernardes, L. R. Londe, E. Soriano, and L. B. L. Santos, "A computational index to expose vulnerabilities in transport infrastructure and socio-environmental disasters: From susceptibility areas analysis to monitoring coverage," *IEEE Latin Amer. Trans.*, vol. 16, no. 5, pp. 1454–1459, May 2018.
- [46] D. Ouyang, X. Zhu, X. Liu, R. He, and Q. Wan, "Spatial differentiation and driving factor Analysis of urban construction land change in county-level city of Guangxi, China," *Land*, vol. 10, no. 7, 2021, Art. no. 691.
- [47] G. Wang and W. Peng, "Quantifying spatiotemporal dynamics of vegetation and its differentiation mechanism based on geographical detector," *Environ. Sci. Pollut. Res.*, vol. 29, no. 21, pp. 32016–32031, 2022.
- [48] B. Ma, S. Wang, C. Mupenzi, H. Li, J. Ma, and Z. Li, "Quantitative contributions of climate change and human activities to vegetation changes in the Upper White Nile River," *Remote Sens.*, vol. 13, no. 18, 2021, Art. no. 3648.
- [49] B. Matlhodi, P. K. Kenabatho, B. P. Parida, and J. G. Maphanyane, "Analysis of the future land use land cover changes in the Gaborone dam catchment using CA-Markov model: Implications on water resources," *Remote Sens.*, vol. 13, no. 13, 2021, Art. no. 2427.
- [50] Y. Ding, T. Ye, and K. Chen, "Analysis of spatio-temporal dynamics and driving forces of vegetation cover in the Hutuo River Basin based on the geographic detector," *Chin. J. Eco-Agriculture*, vol. 30, no. 11, pp. 1737–1749, 2022.
- [51] J.-F. Wang, T.-L. Zhang, and B.-J. Fu, "A measure of spatial stratified heterogeneity," *Ecological Indicators*, vol. 67, pp. 250–256, 2016.
- [52] X. Deng, S. Hu, and C. Zhan, "Attribution of vegetation coverage change to climate change and human activities based on the geographic detectors in the Yellow River Basin, China," *Environ. Sci. Pollut. Res.*, vol. 29, no. 29, pp. 44693–44708, 2022.
- [53] J. Yuan, Y. Xu, J. Xiang, L. Wu, and D. Wang, "Spatiotemporal variation of vegetation coverage and its associated influence factor analysis in the Yangtze River Delta, eastern China," *Environ. Sci. Pollut. Res.*, vol. 26, pp. 32866–32879, 2019.
- [54] L. V. Alexander et al., "Global observed changes in daily climate extremes of temperature and precipitation," *J. Geophysical Res.: Atmospheres*, vol. 111, no. D5, 2006.
- [55] J. F. Siegmund, M. Wiedermann, J. F. Donges, and R. V. Donner, "Impact of temperature and precipitation extremes on the flowering dates of four German wildlife shrub species," *Biogeosciences*, vol. 13, no. 19, pp. 5541–5555, 2016.
- [56] A. J. Felton and M. D. Smith, "Integrating plant ecological responses to climate extremes from individual to ecosystem levels," *Philos. Trans. Roy. Soc. B, Biol. Sci.*, vol. 372, no. 1723, 2017, Art. no. 20160142.
- [57] D. Ye, Z. Guan, S. Sun, X. Li, and Y. Xia, "The relationship between heavy precipitation in the middle and lower reaches of Yangtze River and baroclinic wave packets in the upper troposphere during the Meiyu period of 2016," *Acta Meteorologica Sinica*, vol. 77, no. 1, pp. 73–83, 2019.
- [58] C. Xu, N. G. McDowell, R. A. Fisher, L. Wei, and R. S. Middleton, "Increasing impacts of extreme droughts on vegetation productivity under climate change," *Nature Climate Change*, vol. 9, no. 12, pp. 948–953, 2019.
- [59] X. Zhao, Y. Wang, and T. Zhao, "Spatiotemporal variation and driving factors for FVC in Huaihe River Basin from 1987 to 2021," *Trans. Chin. Soc. Agricultural Machinery*, vol. 54, no. 4, pp. 180–190, 2023.
- [60] Z. Sun, J. Zhang, X. Liu, Z. Tong, D. Yan, and C. Wang, "Quantitative evaluation of drought-flood abrupt alternation during the flood season in Fuyang, China," in *Proc. Intell. Syst. Decis. Mak. Risk Anal. Crisis Response, 4th Int. Conf. Risk Anal. Crisis Response*, 2013, Art. no. 477.
- [61] Fuyang Municipal People's Government. In recent years, the planting area of poplars in our city has decreased significantly. [EB/OL]. May 6, 2022. [Online]. Available: <https://www.fy.gov.cn/content/detail/627481f0886688493a8b456f.html>
- [62] W. Liu et al., "Study on the concentration of top air pollutants in Xuzhou City in winter 2020 based on the WRF-Chem and ADMS-urban models," *Atmosphere*, vol. 15, no. 1, 2024, Art. no. 129.
- [63] X. Qian, D. Wang, J. Wang, S. Chen, and R. G. Eggert, "Resource curse, environmental regulation and transformation of coal-mining cities in China," *Resour. Policy*, vol. 74, Dec. 2021, Art. no. 101447.
- [64] Xinmin Evening News. The Municipal Green Rong Bureau announced the "green figures" to highlight the changes in the past ten years, and the goal of "City of a Thousand Gardens" has been completed more than halfway. [EB/OL]. Oct. 10, 2022. [Online]. Available: <https://baijiahao.baidu.com/s?id=1746260104220762064&wfr=spider&for=pc>
- [65] Y. Zhou, X. Li, and Y. Liu, "Cultivated land protection and rational use in China," *Land Use Policy*, vol. 106, 2021, Art. no. 105454.
- [66] J. Guo, X. Wang, Y. Fan, X. Liang, H. Jia, and L. Liu, "How extreme events in China would be affected by global warming—Insights from a bias-corrected CMIP6 ensemble," *Earth's Future*, vol. 11, no. 4, 2023, Art. no. e2022EF003347.
- [67] M. Xiao, Q. Zhang, V. P. Singh, and X. Chen, "Probabilistic forecasting of seasonal drought behaviors in the Huai River basin, China," *Theor. Appl. Climatol.*, vol. 128, pp. 667–677, 2017.
- [68] K. Venkatesh et al., "Optimal ranges of social-environmental drivers and their impacts on vegetation dynamics in Kazakhstan," *Sci. Total Environ.*, vol. 847, 2022, Art. no. 157562.
- [69] H. Zhao, Z. Yang, L. Li, and L. Di, "Improvement and comparative analysis of indices of crop growth condition monitoring by remote sensing," *Trans. Chin. Soc. Agricultural Eng.*, vol. 27, no. 1, pp. 243–249, 2011.
- [70] K. Shi et al., "Evaluating the ability of NPP-VIIRS nighttime light data to estimate the gross domestic product and the electric power consumption of China at multiple scales: A comparison with DMSP-OLS data," *Remote Sens.*, vol. 6, no. 2, pp. 1705–1724, 2014.
- [71] D. Lu, Y. Wang, Q. Yang, K. Su, H. Zhang, and Y. Li, "Modeling spatiotemporal population changes by integrating DMSP-OLS and NPP-VIIRS nighttime light data in Chongqing, China," *Remote Sens.*, vol. 13, no. 2, 2021, Art. no. 284.



Xueru Tian received the B.S. degree in geographical science from Xinzhou Normal University, Xinzhou, China, in 2022. She is currently working toward the master's degree in geography with Nanjing University of Information Science and Technology, Nanjing, China.

She has been working on the research of dynamic change of fractional vegetation coverage.



Zui Tao was born in China in 1984. He received the B.S. degree from Henan University, Kaifeng, China, the M.S. degree from Wuhan University, Wuhan, China, and the Ph.D. degree from the Institute of Remote Sensing and Digital Earth, Chinese Academy of Sciences (CAS), Beijing, China, all in cartography and geographic information system in 2005, 2008, and 2012, respectively.

He is an Associate Professor with the Aerospace Information Research Institute, CAS. His research interests include validation of remote sensing product, ecological, and environmental remote sensing.



Wen Shao received the B.E. degree in electronics and communication engineering and the M.Eng. degree in communication engineering from Nanjing University of Information Science and Technology, Nanjing, China, in 2017 and 2020, respectively, where he is currently working toward the doctoral degree in 3S integration and meteorological applications.

He has been working on the research of satellite sensor on-orbit radiometric calibration.



Yong Xie (Senior Member, IEEE) received the B.S. and M.S. degrees in physics from the Nanjing Normal University, Nanjing, China, in 2000 and 2004, respectively, and the Ph.D. degree in earth science and geoinformation system from George Mason University, Fairfax, VA, USA, in 2009.

He is currently a Professor with the School of Geographical Science, Nanjing University of Information Science and Technology, Nanjing, China. He has worked on the radiometric calibration and characterization of satellite remote sensor and science product validation with ground measurements.



Shiyu Zhang received the B.S. degree in geographic information science from Nanjing University of Information Science and Technology, Nanjing, China, in 2022, where she is currently working toward the M.S. degree in geography.

She has been focusing on agricultural remote sensing for rice identification and monitoring.